

High-dimensional Bayesian Optimization of Hyperparameters for an Attention-based Network to Predict Materials Property: a Case Study on CrabNet using Ax and SAASBO

Sterling G. Baird^{a,*}, Marianne Liu^{a,b}, Taylor D. Sparks^a

^a*Department of Materials Science and Engineering, University of Utah, Salt Lake City, UT 84108, USA*

^b*West High School, Salt Lake City, Utah 84112, USA*

Abstract

Expensive-to-train deep learning models can benefit from an optimization of the hyperparameters that determine the model architecture. We optimize 23 hyperparameters of a materials informatics model, Compositionally-Restricted Attention-Based Network (CrabNet), over 100 adaptive design iterations using two models within the Adaptive Experimentation (Ax) Platform. This includes a recently developed Bayesian optimization (BO) algorithm, sparse axis-aligned subspaces Bayesian optimization (SAASBO), which has shown exciting performance on high-dimensional optimization tasks. Using SAASBO to optimize CrabNet hyperparameters, we demonstrate a new state-of-the-art on the experimental band gap regression task within the materials informatics benchmarking platform, Matbench ($\sim 4.5\%$ decrease in mean absolute error (MAE) relative to incumbent). Characteristics of the adaptive design scheme as well as feature importances are described for each of the Ax models. SAASBO has great potential to both improve existing surrogate models, as shown in this work, and in future work, to efficiently discover new, high-performing materials in high-dimensional materials science search spaces.

Keywords: sparse axis-aligned subspaces, Bayesian optimization, compositionally restricted attention based network, CrabNet, SAASBO, materials informatics, structure-property model, machine learning

1. Introduction

Bayesian optimization (BO) is an iterative sequential learning¹ algorithm that simultaneously improves model accuracy through exploration of high-uncertainty regions and exploitation of high-performing parameter combinations. It is best-suited for expensive-to-evaluate models with a limited budget of design iterations, and has seen increasing usage in materials informatics [1–7].

In materials informatics, many structure-

property regression and classification models have been developed to accelerate understanding and design of new materials. Compositionally-Restricted Attention-Based Network (CrabNet) is one such model that leverages the transformer network architecture popularized in natural language processing (e.g. text prediction) [8]. The self-attention mechanism allows components (e.g. periodic elements, words) to be interpreted in the context of other components. For example, how does oxygen behave in the context of aluminum vs. nitrogen? How does the word bat behave in the context of cave vs. baseball? CrabNet has achieved state-of-the-art performance on several materials informatics benchmark datasets while only relying composition alone, whereas competing algorithms benefit from having structural features as well.

*Corresponding author.

Email addresses: sterling.baird@utah.edu (Sterling G. Baird), sparks@eng.utah.edu (Taylor D. Sparks)

¹This is also referred to as adaptive design and active learning.

Hyperparameter optimization can be used to improve model performance through optimization of model hyperparameters such as number of layers in a neural network, depth of a random forest, learning rates, and number of training epochs. Many hyperparameter optimization algorithms exist which can be used to tune materials informatics models: grid search, random sampling, Sobol sampling, genetic algorithms, and BO (in order of decreasing iteration “budget” constraints) as well to search through computational [3, 6] and experimental [5, 7, 9–15] materials design spaces. For example, Zhang et al. [16] used a grid search to tune a random forest algorithm to predict Vickers hardness and Dunn et al. [17] used a genetic algorithm to search through extensive combinations of compositional and/or structural features and model architectures to create a general purpose materials informatics algorithm.

Because training deep learning architectures such as CrabNet is an expensive-to-evaluate process, here we focus on BO. To our knowledge², sophisticated hyperparameter optimization has never been performed on CrabNet before and is rare for materials informatics deep learning models, again since they are usually already expensive to train. We note that CrabNet recently achieved state-of-the-art predictive performance on a materials science benchmark within the Matbench framework [17] on the experimental band gap (`matbench_expt_gap`) task [18]. `matbench_expt_gap` is a composition-based (i.e. chemical formula as inputs) regression task consisting of 4604 literature-based datapoints and 5 cross-validation (CV) folds. For additional information, please refer to the Matbench publication Dunn et al. [17] and the <https://matbench.materialsproject.org/> [19].

In this work, we pose the question:

For a model that already exhibits state-of-the-art performance, to what extent can the predictive performance benefit from

²Manual hyperparameter tuning was employed during the initial development of CrabNet.

hyperparameter optimization?

We choose to focus on CrabNet and `matbench_expt_gap` as the case study for hyperparameter optimization because it exhibits state-of-the-art performance without sophisticated hyperparameter optimization and because of our familiarity with the internals of the CrabNet architecture and codebase. Other sophisticated compositional models such as RooSt [20] and Element [21, 22] as well as a variety of other advanced compositional and structure-based regression and classification models (e.g. [8, 17, 23–30]) could have been used with compatible datasets instead.

2. Methods

We describe two models that we use from the Ax Bayesian Optimization framework (Gaussian process expected improvement and sparse axis-aligned subspaces Bayesian optimization (SAASBO)) (Section 2.1), the `matbench_expt_gap` dataset and Matbench nested CV scheme (Section 2.2), and the CrabNet hyperparameters that we chose to optimize (Section 2.3). We summarize the methods in Figure 1.

2.1. Ax Bayesian Optimization

Of the many excellent packages for BO, we choose the Adaptive Experimentation (Ax) platform due to its relative ease-of-use, modularity, developer support, and model sophistication. We refer to this as Ax. In particular, we utilize two models from Ax.

First is a single task Gaussian process regression model with automatic relevance determination (which allows for feature importances), a Matérn 5/2 kernel, and an expected improvement acquisition function (<https://ax.dev/docs/models.html>). We refer to this model as GPEI.

Second is a recently introduced high-dimensional BO scheme: SAASBO [31] which “places strong priors on the inverse lengthscales to avoid overfitting in high-dimensional spaces” and performs well even on problems with hundreds of dimensions [32]. Eriksson and Jankowiak [31] demonstrated

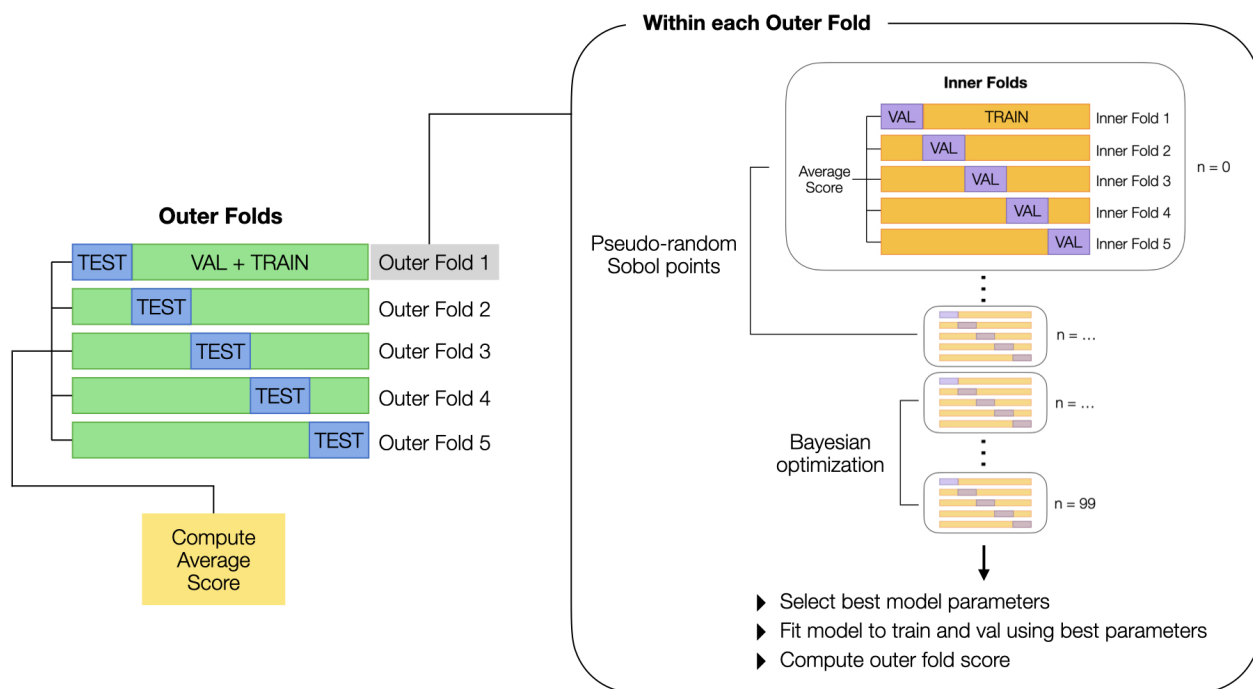


Figure 1: Schematic for Bayesian optimization (BO), including the nested cross-validation (CV) method. For each of the five outer folds, an adaptive design budget of 100 iterations is used to find optimal hyperparameters. The loss function for the hyperparameter optimization is the average score of the five inner folds. The scores are composed of the mean absolute error (MAE) for the validation data divided by the MAE of a dummy regressor (mean absolute deviation) which allows for comparison across different materials science tasks. The optimization starts out with a pseudo-random Sobol point generation phase followed by a Bayesian optimization phase. The Sobol points exist to create a rough initial model prior to Bayesian optimization, consistent with convention and for performance reasons. After the Bayesian optimization is complete, the hyperparameter combination with the best averaged inner score is selected, and a model is refitted to both the training and validation data, with the outer fold score computed based on the outer fold test set. This process is repeated for the other four outer folds, finally resulting in an averaged outer fold score. This final score (along with other metadata and statistics) is reported on the Matbench website. Nested CV is computationally expensive but helps ensure model generalizability and comparability with other models. This figure is inspired by <https://hackingmaterials.lbl.gov/automatminer/advanced.html>.

that SAASBO outperforms a slew of other high-dimensional optimization algorithms on a variety of general machine learning tasks. We are excited to bridge this model’s use to the field of materials informatics which is rich in adaptive design problems. We refer to this model as SAASBO.³

For both models, we allow the model to infer noise levels rather than imposing a constant noise as an *a-priori* constraint or standard deviations supplied on a per-datapoint basis during the optimization⁴; however, Ax is capable of handling these and other tasks including multi-objective optimization, risk-averse BO, batch-wise optimization, and custom surrogate models as well as a variety of other non-algorithm related features⁵. Because the computational overhead of SAASBO scales cubically with the number of datapoints, it is typically limited to several hundred adaptive design iterations which is appropriate for our expensive hyperparameter optimization use-case.

One-hundred sequential design iterations were used for both models. For GPEI and SAASBO, $2 \times n$ (where n is the number of parameters) and 10 initial (quasi-random) Sobol⁶ iterations were used to create a rough initial model, respectively. These choices are consistent with convention and defaults within Ax.

³23 hyperparameters might not seem large at first; but for a design budget of only 100 iterations, finding optimal hyperparameter is a difficult problem.

⁴Repeat measurements may also be supplied directly rather than imposing the assumption of a particular noise distribution, e.g. Gaussian.

⁵Examples of non-algorithm related features within Ax are field experiments (e.g. wetlab experimental adaptive design) and interfacing with external databases.

⁶Sobol sequences are a quasi-random sampling method that produces relatively equally spaced points across all dimensions compared with both random search and grid search. Random search tends to do well at avoiding systematic biases in the distance as with grid search; however, certain regions may still be sparsely populated. Sobol sequences tend to produce higher quality searches than both random and grid searches (this may be especially true for high-dimensional spaces). Sobol sequences are constrained to 2^m sampling points, where m is a non-negative integer. For more information, see `scipy.stats.qmc.Sobol (v1.8.0)`

2.2. Data and Validation

As mentioned earlier (Section 1), we choose the experimental band gap Matbench dataset [17, 18] (`matbench_expt_gap`), a composition-based regression task consisting of 4604 literature-based datapoints and 5 CV outer folds. Additionally, we perform nested CV such that hyperparameter optimization iterations are performed based on minimizing the average MAE across each of the five inner folds (this is the Ax objective). The best parameter set was then trained on all the inner fold data and used to predict on the test set (never before seen during training or hyperparameter optimization). In pseudo-code, this appears as follows:

```
for outer_fold in outer_folds:
    for iteration in iterations:
        for inner_fold in inner_folds:
            compute score
            compute average score
        select best model parameters
        train model using best parameters
        compute score
    compute average score
```

For the inner folds, we follow the Matbench recommendation (<https://hackingmaterials.lbl.gov/automatminer/datasets.html>) of using the following inner CV folds⁷:

```
from sklearn.model_selection import KFold
kf = KFold(
    n_splits=n_splits,
    shuffle=True,
    random_state=18012019,
)
for train_index, val_index in kf.split(
    train_val_df
):
    train_df, val_df = (
        train_val_df.loc[train_index],
        train_val_df.loc[val_index],
    )
```

For a single matbench task, CrabNet undergoes model instantiation and fitting $5 \times 5 \times 100 = 2500$ times. Use of nested CV helps ensure that the model results are both generalizable and comparable with other models. The nested CV results bol-

⁷The code was formatted in Black code style via an online formatter: <https://black.vercel.app/>.

ster our confidence that the results in this work are both reproducible⁸ and generalizable to in-domain experimental band gap predictions. While effective, nested CV is also computationally expensive. With relatively sophisticated graphical processing units (e.g. NVIDIA 2080-Ti), nested CV for `matbench_expt_gap` using CrabNet predictions takes over a day to complete and resides somewhere in the gray area between requiring consumer hardware vs. high-performance computing. See [Automatminer: running a benchmark](#) and Dunn et al. [17] for more information on nested CV.

2.3. CrabNet hyperparameters

We use two Ax Bayesian adaptive design models (Section 2.1) to simultaneously optimize 23 hyperparameters of CrabNet (Table 1). Parameters were surfaced in the top-level application programming interface (API) from several thousand lines of nested code within CrabNet, and search space constraints were imposed based on a combination of intuition and algorithm/data constraints. Some trial-and-error was involved to figure out invalid combinations of hyperparameters. For example, the model architecture dimensions (`d_model`) needed to be divisible by the number of attention heads (`heads`). As another example, the `jarvis`, `olinyk`, and `ptable` elemental featurizers (`elem_prop` keyword argument) were eliminated either due to an incomplete representation of elements contained in `matbench_expt_gap` chemical formulas or an incompatible datatype (in our case, `string`).

An additional consideration is that certain CrabNet hyperparameters required reparameterization to be compatible with the Ax API or remove degenerate dimensions. We give an example of each.

As an example of API compatibility, the number of hidden dimensions in the CrabNet recurrent neural network (`out_hidden`) is passed as a list of integers whereas the Ax API would require each of these integers as individual parameters. In this case for both API compatibility and simplicity, we chose

the last integer in this list as `out_hidden4` and chose the size of the preceding three layers as twice the size of the next layer (e.g. [1024, 512, 256, 128]). Likewise, `betas` was split into `betas1` and `betas2` with the constraint that `betas1 < betas2`.

As an example of removing degenerate dimensions, the embedding, fractional prevalence encoding, and log fractional prevalence encoding undergo a weighted average via `emb_scaler`, `pe_scaler`, and `ple_scaler`, respectively. Despite having three parameters associated with them, this search subspace has only two non-degenerate dimensions (degrees-of-freedom) due to the normalization linear equality constraint of the weighted average (`emb_scaler + pe_scaler + ple_scaler == 1`). Imposing equality constraints can lead to numerical instabilities for optimization schemes that rely on volume-based sampling, so in the reparameterization, this is represented without the degenerate dimension as an inequality constraint (`emb_scaler + pe_scaler <= 1`). This is an important aspect of preventing unnecessarily large search spaces in an already high-dimensional optimization scheme.

We note that in addition to the rules mentioned in this section, `epochs` was set to $4 \times \text{epochs_step}$ during reparameterization and `heads` was constrained to be even except in the case that `heads==1`. For a full workflow of the reparameterization procedure, see <https://github.com/spark-s-baird/crabnet-hyperparameter/blob/b720d5fd6cadb286079dc8c49c1a5733e263585e/utils/parameterization.py#L10-L48>.

A summary of the 23 CrabNet hyperparameters optimized in this work is presented in Table 1.

3. Results and Discussion

We discuss improvements in model performance offered by GPEI and SAASBO models relative to a baseline model (Section 3.1) and analyze the characteristics of the hyperparameter optimization across iterations and for individual hyperparameters (Section 3.2). Finally, we discuss future work (Section 3.3).

⁸Our remark about reproducibility assumes that the specified software versions for CrabNet, Matbench, and each of their dependencies are used.

Table 1: Table of 23 CrabNet parameter names, ranges/possible values, short description, and default parameter values. FC stands for fully-connected.

Parameter	Min.	Max.	Default	Description
N	1	10	3	Number of attention layers
alpha	0.0	1.0	0.5	Lookahead “slow update” rate
bias	[False, True]		False	Whether to bias residual network
criterion	[“RobustL1”, “RobustL2”]		“RobustL1”	Loss function
d_model	100	1024	512	FC network output dimension
dim_feedforward	1024	4096	2048	Feedforward network dimension
dropout	0.0	1.0	0.1	Feedforward dropout fraction
elem_prop	[“mat2vec”, “magpie”, “onehot”]		“mat2vec”	Elemental feature vector
emb_scaler	0.0	1.0	1.0	Elemental embeddings weight
epochs_step	5	20	10	Step size of epochs
eps	0.0000001	0.0001	0.000001	Prevents zero-division in LAMB
fudge	0.0	0.1	0.02	Jitter to fractional encodings
heads	1	10	4	Number of attention heads
k	2	10	6	Number of Lookahead steps
lr	0.0001	0.006	0.001	Learning rate
pe_resolution	2500	10000	5000	Prevalence encoding resolution
ple_resolution	2500	10000	5000	Prevalence log encoding resolution
pos_scaler	0.0	1.0	1.0	Fractional encodings weight
weight_decay	0.0	1.0	0	L2 penalty in LAMB
batch_size	32	256	32	Training batch size
out_hidden4	32	512	128	4th layer size of residual network
betas1	0.5	0.9999	0.9	Gradient coefficient in LAMB
betas2	0.5	0.9999	0.999	Squared gradient coefficient in LAMB

3.1. Improvement in Model Performance

GPEI hyperparameter optimization resulted in a moderate performance improvement relative to the default CrabNet hyperparameters⁹. Notably, SAASBO hyperparameter optimization exhibited nearly twice the performance improvement compared to the improvement of GPEI over default hyperparameters. Additionally, SAASBO set the new state-of-the-art benchmark for `matbench_expt_gap`, which further strengthens its evidence as an effective high-dimensional Bayesian optimization scheme. We summarize the predictive performance of GPEI, SAASBO, and our baseline model against other Matbench submissions in Figure 2 and Table 2. As of 2022-03-16, the results of this work are available on the [Matbench leaderboard website](#) [19] under “Leaderboards Per Task” for `matbench_expt_gap`. Reproducible scripts are made available in the Matbench GitHub repository under the `benchmarks` directory (<https://github.com/materialsproject/matbench>).

3.2. Hyperparameter Optimization

We describe characteristics of the hyperparameter optimization results for both GPEI and SAASBO models in the context of best parameter combinations as a function of iteration (Section 3.2.1), interpretable model characteristics such as the selected hyperparameter combinations and feature importances (Section 3.2.2), and CV results for the predicted vs. actual CrabNet MAEs (Section 3.2.3).

3.2.1. Best Objective vs. Iteration

Best objective vs. iteration plots for GPEI and SAASBO are shown for each Matbench fold in Figure 3 and Figure 4, respectively. The first 46 GPEI Sobol points have a large scatter, but improve the accuracy of the internal Gaussian process regression model.

At iteration 47, the Bayesian optimization iterations begin, at which point the MAEs have a much tighter spread.

In the case of SAASBO, only 10 initial Sobol points are used, consistent with convention within Ax. We

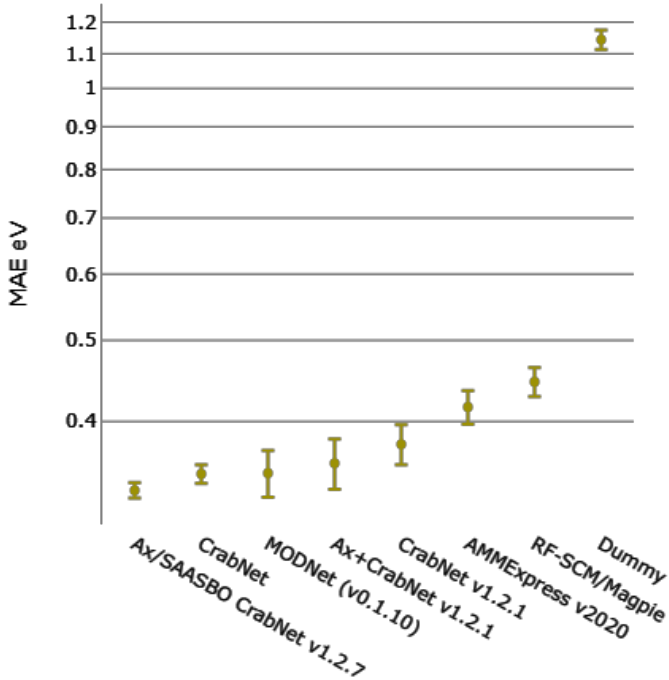


Figure 2: Comparison of mean MAE (eV) with standard deviation MAE (eV) across five folds for CrabNet v1.2.1 with default hyperparameters, Ax+CrabNet v1.2.1, Ax/SAASBO CrabNet v1.2.7, and other matbench submissions on the `matbench_expt_gap` v0.1 task. The CrabNet submission (`mae==0.3463`) was submitted by a separate party, likely with a large number of epochs (e.g. `epochs==300`) relative to the upper limit of `epochs` (80) in this work. As of 2022-03-16, the results shown in this figure are available on the [Matbench leaderboard website](#) [19] under “Leaderboards Per Task” for `matbench_expt_gap`.

⁹Manual trial and error was used to tune CrabNet hyperparameters prior to publication of CrabNet [8].

Table 2: Comparison of mean MAE, standard deviation of MAE, mean root-mean-square error, and max `max_error` across five folds for `CrabNet v1.2.1` with default hyperparameters, `Ax+CrabNet v1.2.1`, `Ax/SAASBO CrabNet v1.2.7`, and other `matbench` submissions on the `matbench_expt_gap v0.1` task. `CrabNet` submission (`mae==0.3463`) was submitted by a separate party, likely with a large number of epochs (e.g. `epochs==300`) relative to the upper limit of `epochs` (80) in this work. As of 2022-03-16, the results shown in this figure are available on the [Matbench leaderboard website](#) [19] under “Leaderboards Per Task” for `matbench_expt_gap`.

algorithm	mean mae (eV)	std mae (eV)	mean rmse (eV)	max max_error (eV)
Ax/SAASBO CrabNet v1.2.7	0.3310	0.0071	0.8123	11.1001
CrabNet	0.3463	0.0088	0.8504	9.8002
MODNet (v0.1.10)	0.3470	0.0222	0.7437	9.8567
Ax+CrabNet v1.2.1	0.3566	0.0248	0.8673	11.0998
CrabNet v1.2.1	0.3757	0.0207	0.8805	10.2572
AMMExpress v2020	0.4161	0.0194	0.9918	12.7533
RF-SCM/Magpie	0.4461	0.0177	0.8243	9.5428
Dummy	1.1435	0.0310	1.4438	10.7354

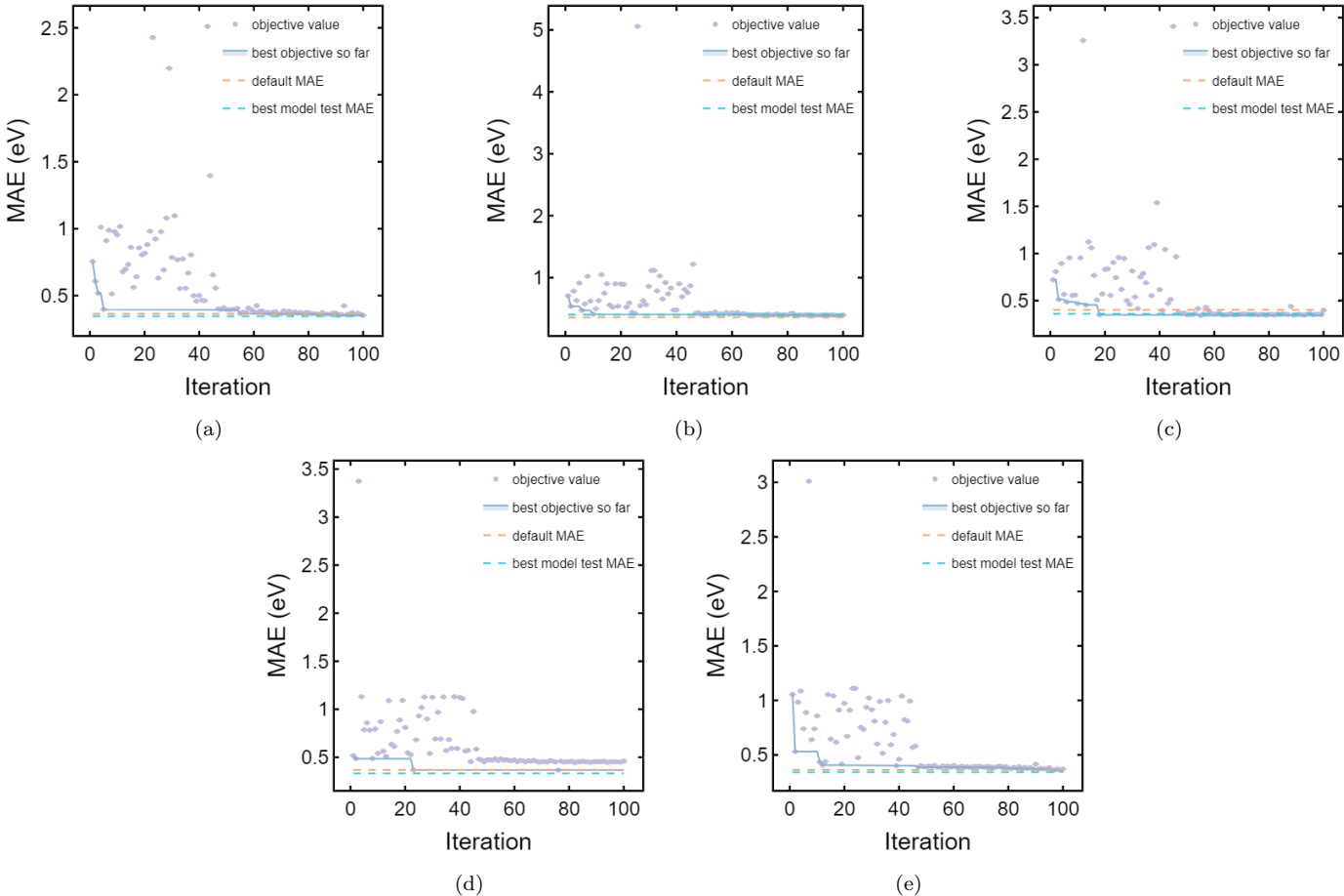


Figure 3: Best objective vs. GPEI optimization iteration for each of the five `matbench_expt_gap` folds. First 46 iterations are Sobol points.

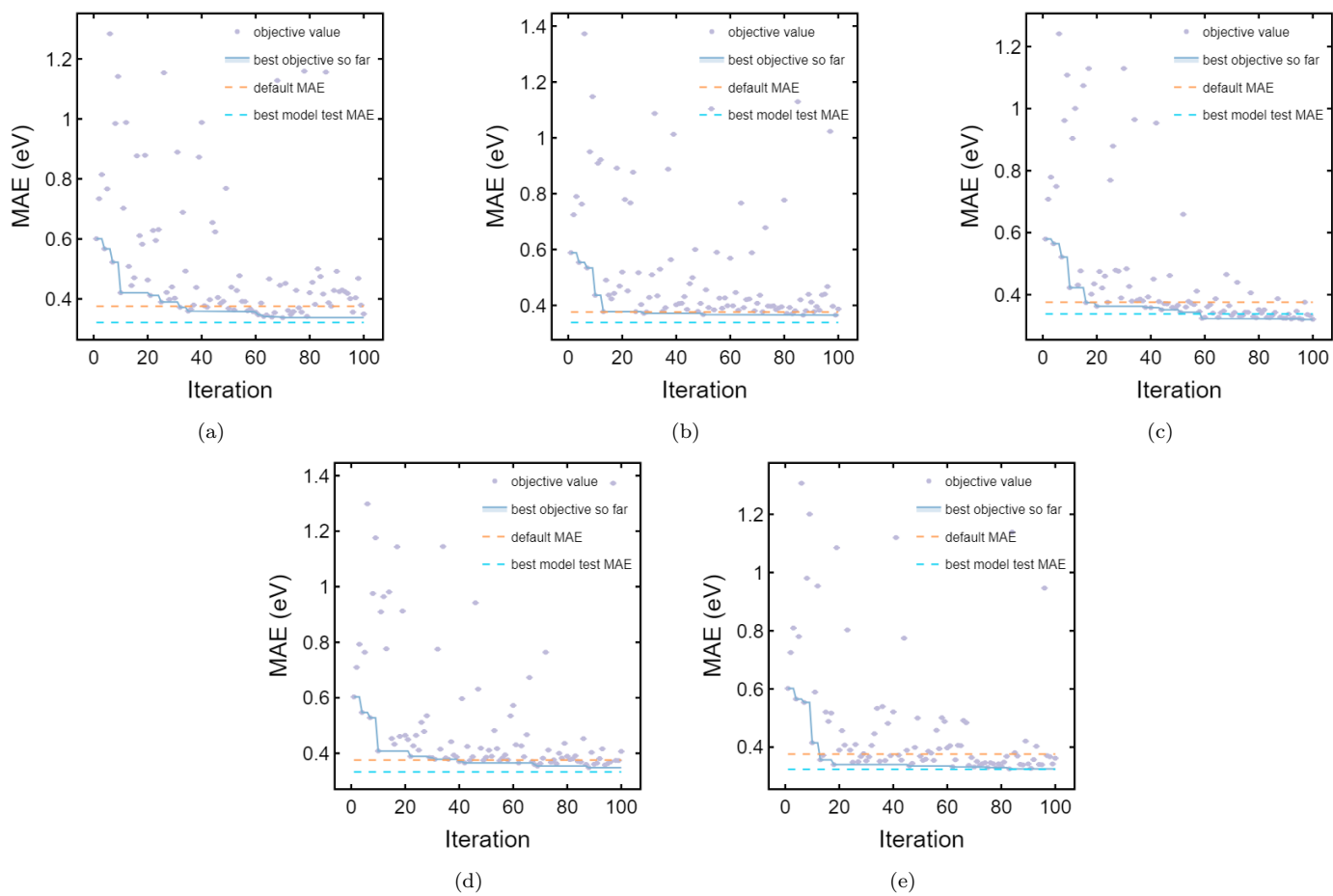


Figure 4: Best objective vs. SAASBO optimization iteration for each of the five `matbench_expt_gap` folds. First 10 iterations are Sobol points.

notice that during the SAASBO iterations, there is a much larger spread in MAE than with GPEI indicating perhaps that SAASBO is less likely to get trapped searching in a local minimum. In other words, SAASBO seems to favor exploration more than GPEI during later iterations.

We also note that in every SAASBO `matbench_expt_gap` fold, the best model test MAE is better than the default MAE, whereas in one case with GPEI the best model test MAE is worse than the default MAE.

3.2.2. Interpretable Model Characteristics

A summary of the best hyperparameter combinations out of 100 iterations for the GPEI and SAASBO models is shown in Table 3. It is interesting to note that in every case, SAASBO pushed the number of epochs to the upper limit of 80, whereas GPEI ranged from 40 to 68. In other words, with a limited budget of 100 iterations, SAASBO seems to have determined that maximizing the number of epochs tends to reduce the test error, especially since CrabNet implements early stopping. While this may be obvious to machine learning practitioners, it is noteworthy that SAASBO identified this trend without prior knowledge other than the user-chosen constraints on the search space.

A summary of the GPEI and SAASBO feature importances with standard deviations across the 5 Matbench folds is given in Figure 5. Relative feature importances for each of the five folds for the two models are given in ?? and ??, respectively. The GPEI feature importances have a more gradual decay compared with the SAASBO features. The minimum and maximum relative feature importances for GPEI are typically $\sim 2\%$ and $\sim 10\%$, respectively, whereas the minimum and maximum relative feature importances for SAASBO range from $\sim 1\%$ to $\sim 25\%$, respectively. This is indicative of the strong priors on the inverse lengthscales within the SAASBO framework and previous results indicating a relatively small number of features being recognized as important to the model as the adaptive design process progresses (see Figure 5. of Eriksson and Jankowiak [31]).

Additionally, we notice that GPEI tends to place much higher weights on the categorical param-

eters than SAASBO and that SAASBO places greater weight on the relative contributions of the embedding, fractional encoding, and log-fractional encoding than GPEI. A commonality between the two methods is that `dropout` tends to be ranked highly in terms of feature importance in either method.

Another interpretable aspect is the plotting of 1D slices through the model parameter space. In this work, we fix all other parameters than the one being varied to the mean and mode of the numerical and categorical parameters across the 100 iterations for each of the models. For `epochs_step`, we notice that in general, SAASBO captures the intuitive trend that as number of training epochs increases, model error decreases until it plateaus due to early stopping better than GPEI. With GPEI, local minima and flatter trends dominate, indicating that the effect of this parameter was not properly learned within the 100 iterations across 23 hyperparameters. The SAASBO results are significant; no *a-priori* information was made available to either of the models excepting the allowed ranges that constrain the search space. In other words, SAASBO identified an important trend with limited observations in a high-dimensional design space. This is further supported by the observation that SAASBO uncertainties are generally tighter for a larger number of epochs than GPEI, which indicates that SAASBO devoted more search power to the regions of the model parameter space with a large number of epochs (which we expect to have favorable performance).

The superiority of SAASBO relative to GPEI in recognizing the true influence of `epochs_step` is well-supported; however, this does not preclude SAASBO from missing important trends and fine details depending on the complexity and dimensionality of the search space as well as the design budget. For interested readers, 1D slices for all 23 parameters for both models across each of the 5 Matbench folds are available in supporting information (??).

3.2.3. Predicted Model Error Cross-validation Results

The leave-one-out cross-validation results for GPEI (Figure 7) and SAASBO (Figure 8) exhibit qualitative differences. For example, the GPEI results tend to exhibit a plateau from 0.4 eV to 1.2 eV and

Table 3: Table of best parameterization for the default values and each of the 5 outer folds for GPEI and SAASBO with the mean absolute error as the last row (25 rows \times 11 cols).

parameter	default	ax_fold_0	ax_fold_1	ax_fold_2	ax_fold_3	ax_fold_4	saas_fold_0	saas_fold_1	saas_fold_2	saas_fold_3	saas_fold_4
N	3	4	5	3	3	6	2	3	4	5	2
alpha	0.500	0.8791	0.7990	0.8042	1.000	0.7345	1.000	0.8019	0.666	0.6209	0.9403
bias	False	True	False	False	True	False	True	False	False	False	False
criterion	RobustL1	RobustL1	RobustL1	RobustL1	RobustL1	RobustL1	RobustL1	RobustL1	RobustL1	RobustL1	RobustL1
d_model	512	860	516	660	940	288	890	690	1024	1024	1024
dim_feedforward	2048	3498	2663	3469	1981	1393	4096	1179	1903	2322	2074
dropout	0.1000	0.2105	0.2226	0.03475	0.003479	0.02590	0.02887	1.79e-15	0.09428	0.0954	0.00e+00
elem_prop	mat2vec	mat2vec	onehot	onehot	mat2vec	mat2vec	mat2vec	onehot	mat2vec	onehot	mat2vec
emb_scaler	1.000	0.2547	0.3182	0.5283	0.6800	0.4326	0.7786	0.2733	0.3257	0.2925	0.6672
epochs	40	40	60	60	68	68	80	80	80	80	80
epochs_step	10	10	15	15	17	17	20	20	20	20	20
eps	1.00e-06	0.00007087	4.48e-05	2.62e-05	0.00008816	3.95e-05	2.78e-05	2.39e-05	1.53e-05	1.00e-07	1.00e-07
fudge	0.02000	0.07413	0.01511	0.08701	0.05812	0.06170	7.93e-08	2.83e-16	0.01194	0.03473	0.00e+00
heads	4	4	6	10	10	8	10	10	2	8	8
k	6	6	2	3	10	5	2	2	6	2	2
lr	0.001000	0.002053	0.002904	0.002141	0.004779	0.004934	0.0003422	0.0001000	0.006	0.001696	0.005231
pe_resolution	5000	7185	8609	7277	6354	5426	2500	5403	2652	8735	2500
ple_resolution	5000	4322	6758	7289	4584	8203	4952	2500	10000	4814	10000
pos_scaler	1.000	0.2043	0.2064	0.1782	0.3012	0.5221	2.47e-07	0.005612	3.01e-12	0.3951	0.3328
pos_scaler_log	1.000	0.5411	0.4754	0.2936	0.01877	0.04523	0.2214	0.7211	0.6743	0.3124	4.78e-10
weight_decay	0	0.1264	0.5729	0.07740	0.7779	0.4129	1.44e-09	2.37e-15	1.10e-13	3.81e-17	0.00e+00
batch_size	256	69	165	63	241	125	32	32	32	104	32
out_hidden0	1024	1584	3048	3720	3392	984	1264	256	256	1904	2904
betas0	0.9000	0.5216	0.6461	0.7111	0.5592	0.5574	0.5166	0.5000	0.5000	0.7642	0.5213
betas1	0.999	0.7118	0.7283	0.9476	0.5830	0.9347	0.5265	0.5000	0.5000	0.7978	0.9999
test MAE	0.3757	0.3465	0.4029	0.3599	0.3324	0.3412	0.3214	0.3385	0.3383	0.3327	0.3239

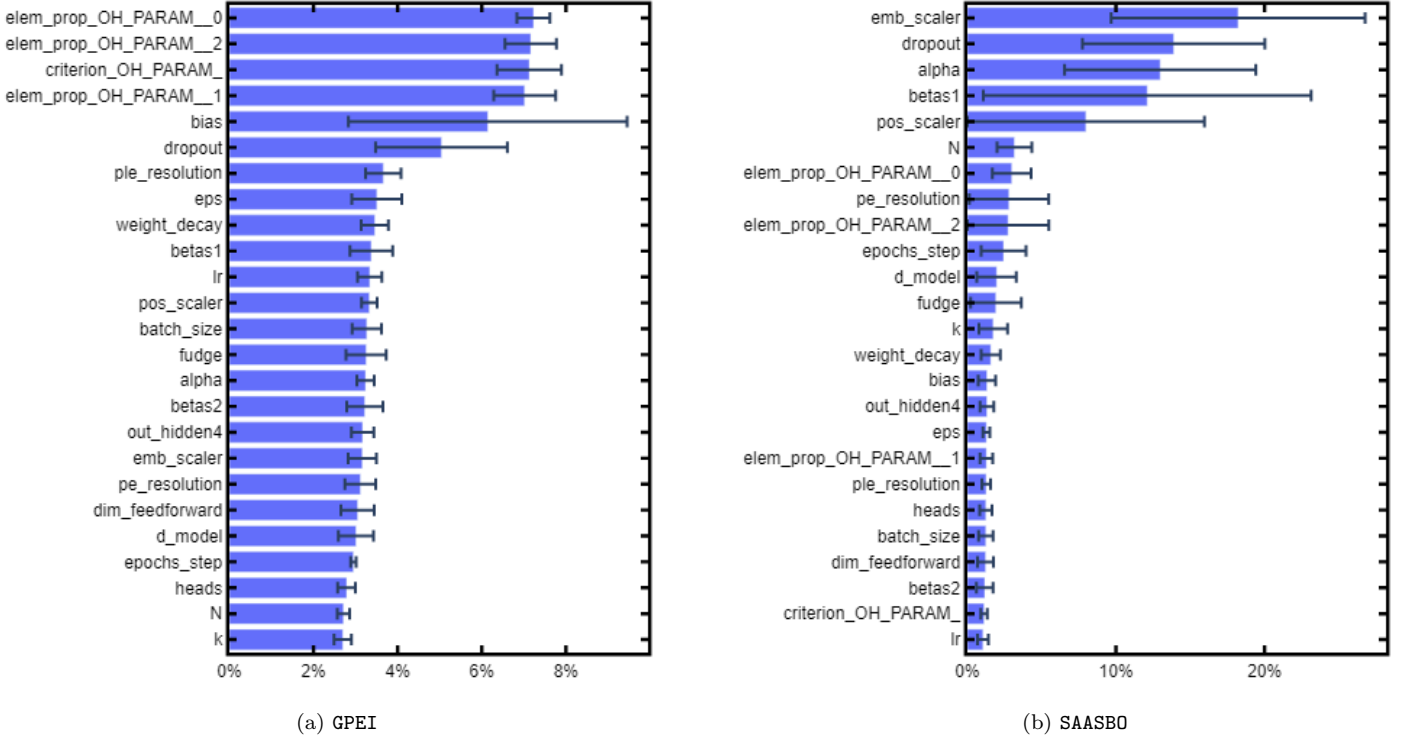


Figure 5: Relative GPEI (a) and SAASBO (b) feature importances of CrabNet hyperparameters averaged over the five `matbench_expt_gap` folds based on data from 100 iterations per fold. For GPEI, the first 46 iterations were Sobol points, and the remaining 54 iterations were Bayesian optimization iterations. For SAASBO, the first 10 iterations were Sobol points, and the remaining 90 iterations were Bayesian optimization iterations. Standard deviations are given as error bars with lower error bars truncated. `_OH_PARAM_#` refers to choices for categorical variables.

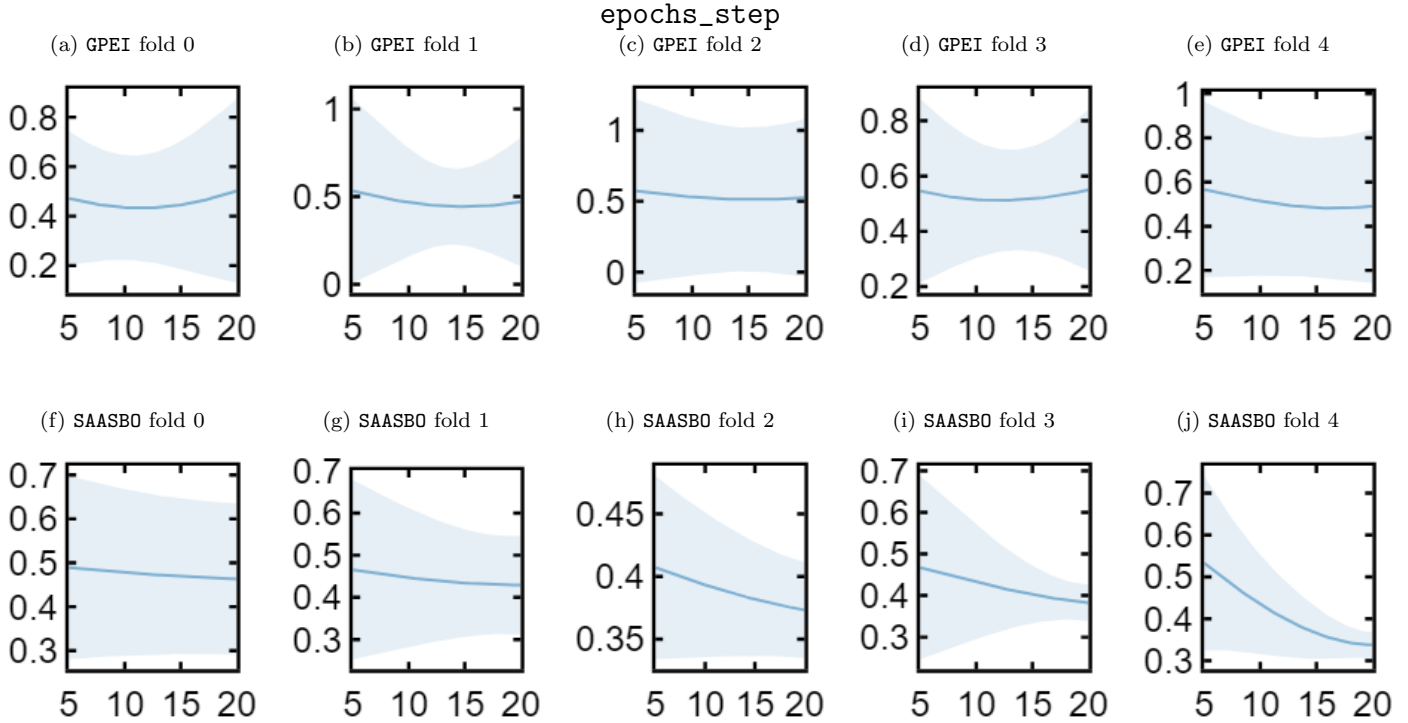


Figure 6: One-dimensional (1D) slices of MAE (eV) vs. `epochs_step` through the GPEI and SAASBO parameter spaces with the rest of the parameters fixed to the mean and mode of the 100 sampled numeric and categorical parameters, respectively, for each of the models.

actual MAE values as large as ~ 5 eV. For SAASBO, there are no distinct plateaus, and the typical maximum actual MAE is ~ 1.5 eV. In general, the GPEI results seem to have a higher frequency of overconfident predictions in the high error regions compared with SAASBO.

3.3. Future Work

A number of questions may be interesting to explore in future work:

- Is the improvement in predictive performance worth the computational and implementation cost?
- How does multi-objective optimization SAASBO perform when also considering root-mean-square error, uncertainty quantification quality (e.g. interval score [33]), model size, and/or computational runtime as additional objectives?

- Does the best combination of hyperparameters for one property (e.g. experimental band gap) retain its superior predictive performance when applied to separate properties (e.g. bulk modulus, hardness, Coulombic efficiency) or different data modalities (computational vs. experimental), or are the best parameterizations specific to the particular optimization task?
- Can CrabNet hyperparameter optimization be successfully framed as an artificial (cheaper-than-density functional theory) materials discovery benchmark task?

While we focus on hyperparameter optimization, SAASBO is also highly applicable to finding extraordinary candidates during materials discovery campaigns assuming a relatively small number of initial datapoints and adaptive design iterations characteristic of many materials discovery tasks. In the near-term, we plan to apply SAASBO to a real materials discovery campaign in comparison with

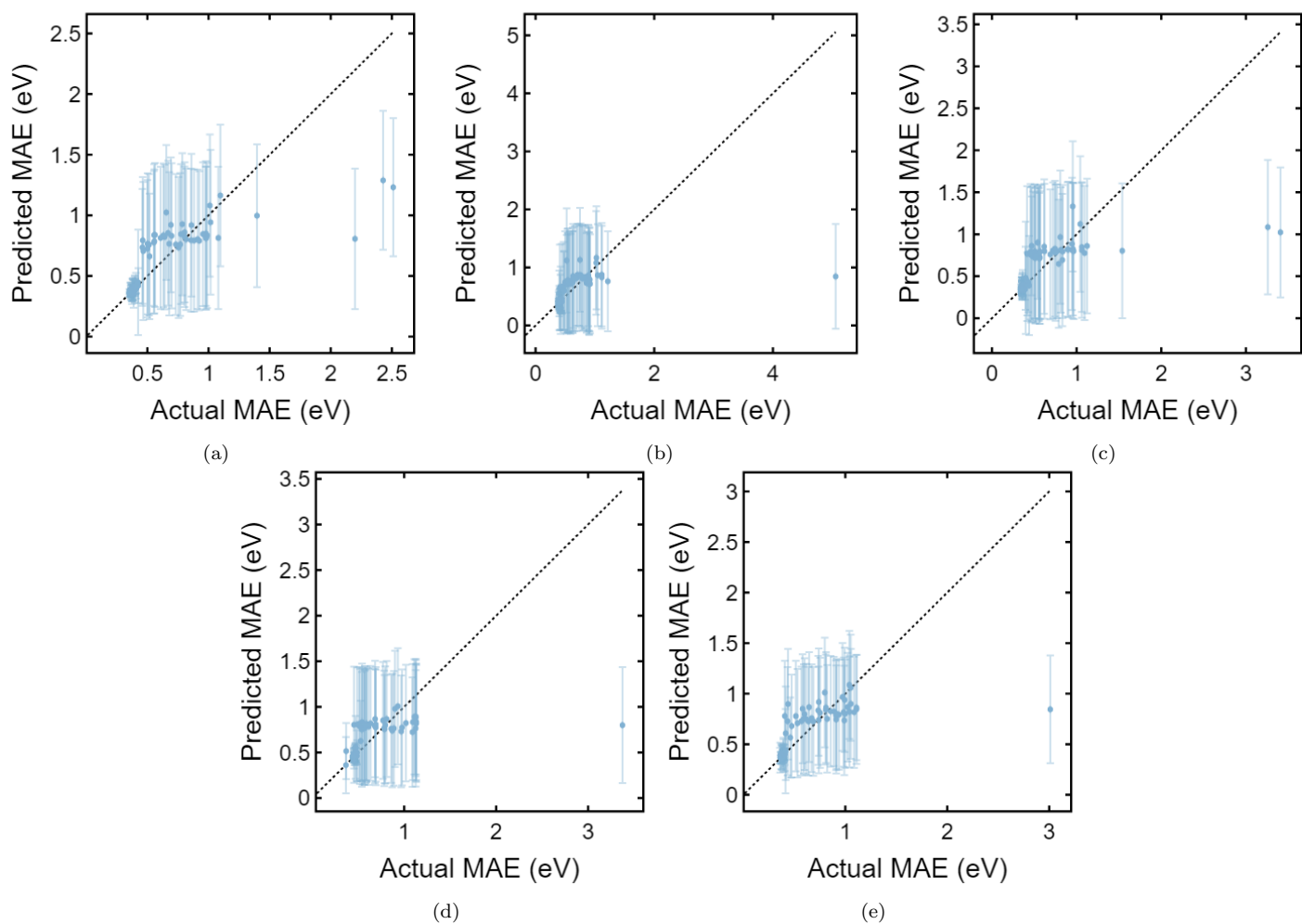


Figure 7: Leave-one-out cross-validation results for GPEI CrabNet hyperparameter combinations for each of the five `matbench_expt_gap`. The first 46 iterations were Sobol points, and the remaining 54 iterations were Bayesian optimization iterations.

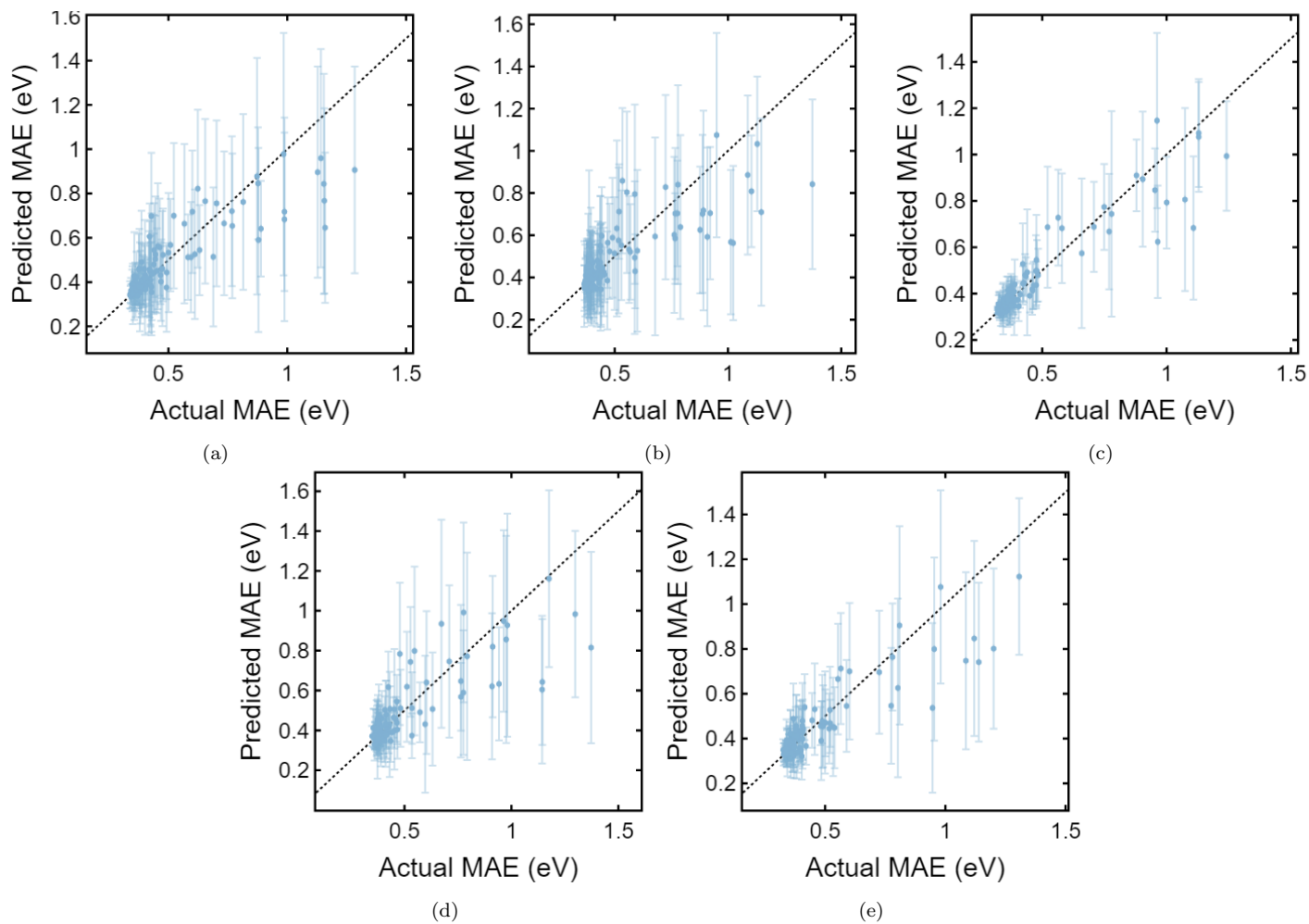


Figure 8: Leave-one-out cross-validation results for SAASBO CrabNet hyperparameter combinations for each of the five `matbench_expt_gap`. The first 10 iterations were Sobol points, and the remaining 90 were SAASBO iterations.

other materials discovery algorithms (Open Citrine Platform [34] and DiSCoVeR [35]).

4. Conclusion

A recently introduced high-dimensional BO scheme (SAASBO) as well as a classical BO scheme are successfully applied to the task of optimizing hyperparameters for a materials informatics model (CrabNet). To illuminate our initially posed question (Section 1), use of SAASBO to optimize CrabNet sets a new state-of-the-art for an experimental band gap regression task (`matbench_expt_gap`) by a margin of ~ 0.015 eV ($\sim 4.5\%$ decrease). In terms of model interpretability, SAASBO successfully identifies number of epochs¹⁰ as a parameter to be maximized; in each of the 5 CV folds, the SAASBO optimized number of epochs reached the limit of the max allowed epochs (80). Additionally, we find that SAASBO seems to favor exploration over exploitation during later design iterations, indicative of the model’s ability to avoid overfitting for high-dimensional problems. We believe that SAASBO and other high-dimensional BO algorithms will accelerate deployment of better materials informatics models and efficient searches in high-dimensional materials discovery design spaces.

Glossary

API application programming interface 5

BO Bayesian optimization 1–4, 15

CrabNet Compositionally-Restricted Attention-Based Network 1, 2, 4–7, 10, 11, 13–15

CV cross-validation 2–5, 7, 15

MAE mean absolute error 1, 3, 4, 7, 8, 10–12

SAASBO sparse axis-aligned subspaces Bayesian optimization 1, 2, 4, 10, 12, 14, 15

¹⁰In CrabNet, early stopping is implemented, and so we expect the performance to eventually plateau as number of epochs is increased.

Conflicts of Interest

There are no conflicts of interest to declare.

Acknowledgement

We thank Anthony Wang for useful discussion on CrabNet hyperparameters. Plots were produced via Plotly [36] and Ax’s plotting wrapper functions. Several tables were formatted via an [online formatter](#) [37] and the [auto-paper methodology](#) [38] was used. This work was supported by the National Science Foundation under Grant No. DMR-1651668.

CRedit Statement

Sterling G. Baird: Supervision, Project administration, Conceptualization, Methodology, Software, Validation, Formal analysis, Investigation, Writing - Original Draft, Writing - Review & Editing, Visualization. **Taylor D. Sparks:** Supervision, Project administration, Funding acquisition, Resources, Writing - Review & Editing. **Marianne Liu:** Methodology, Software, Writing - Review & Editing, Visualization

Data Availability

The raw data required to reproduce these findings is available to download via the python `matbench v0.5` package (<https://pypi.org/project/matbench/0.5/>). The data is also available at <https://hackingmaterials.lbl.gov/automatminer/datasets.html>.

The processed data required to reproduce these findings is available to download from <https://github.com/sparks-baird/crabnet-hyperparameter> as `v0.1.0` [39].

The code required to reproduce these findings is hosted at <https://github.com/sparks-baird/crabnet-hyperparameter> as `v0.1.0` [39].

Additionally, the results are published on the Matbench webpage (https://matbench.materialsproject.org/Leaderboards%20Per-Task/matbench_v0.1_matbench_expt_gap/), and reproducer Jupyter notebooks and full metadata are available on the Matbench GitHub repository (<https://github.com/materialsproject/matbench>) under the `benchmarks` folder.

References

- [1] R. Dong, Y. Dan, X. Li, J. Hu, Inverse Design of Composite Metal Oxide Optical Materials based on Deep Transfer Learning, *Computational Materials Science* 188 (2021) 110166. doi:[10.1016/j.commatsci.2020.110166](https://doi.org/10.1016/j.commatsci.2020.110166). arXiv:[2008.10618](https://arxiv.org/abs/2008.10618).
- [2] R. Espinosa, H. Ponce, J. Ortiz-Medina, A 3D orthogonal vision-based band-gap prediction using deep learning: A proof of concept, *Computational Materials Science* 202 (2022) 110967. doi:[10.1016/j.commatsci.2021.110967](https://doi.org/10.1016/j.commatsci.2021.110967).
- [3] S. Ju, T. Shiga, L. Feng, Z. Hou, K. Tsuda, J. Shiomi, Designing Nanostructures for Phonon Transport via Bayesian Optimization, *Phys. Rev. X* 7 (2017) 021024. doi:[10.1103/PhysRevX.7.021024](https://doi.org/10.1103/PhysRevX.7.021024).
- [4] M. Karasuyama, H. Kasugai, T. Tamura, K. Shitara, Computational design of stable and highly ion-conductive materials using multi-objective bayesian optimization: Case studies on diffusion of oxygen and lithium, *Computational Materials Science* 184 (2020) 109927. doi:[10.1016/j.commatsci.2020.109927](https://doi.org/10.1016/j.commatsci.2020.109927).
- [5] A. Sakurai, K. Yada, T. Simomura, S. Ju, M. Kashiwagi, H. Okada, T. Nagao, K. Tsuda, J. Shiomi, Ultranarrow-Band Wavelength-Selective Thermal Emission with Aperiodic Multilayered Metamaterials Designed by Bayesian Optimization, *ACS Cent. Sci.* 5 (2019) 319–326. doi:[10.1021/acscentsci.8b00802](https://doi.org/10.1021/acscentsci.8b00802).
- [6] A. Talapatra, S. Boluki, T. Duong, X. Qian, E. Dougherty, R. Arróyave, Autonomous efficient experiment design for materials discovery with Bayesian model averaging, *Physical Review Materials* 2 (2018) 113803. doi:[10.1103/PhysRevMaterials.2.113803](https://doi.org/10.1103/PhysRevMaterials.2.113803). arXiv:[1803.05460](https://arxiv.org/abs/1803.05460).
- [7] Y. K. Wakabayashi, T. Otsuka, Y. Krockenberger, H. Sawada, Y. Taniyasu, H. Yamamoto, Machine-learning-assisted thin-film growth: Bayesian optimization in molecular beam epitaxy of SrRuO₃ thin films, *APL Materials* 7 (2019) 101114. doi:[10.1063/1.5123019](https://doi.org/10.1063/1.5123019). arXiv:[1908.00739](https://arxiv.org/abs/1908.00739).
- [8] A. Y.-T. Wang, S. K. Kauwe, R. J. Murdock, D. Sparks, Compositionally-Restricted Attention-Based Network for Materials Property Predictions, *npj Computational Materials* (2021) 33. doi:[10.1038/s41524-021-00545-1](https://doi.org/10.1038/s41524-021-00545-1).
- [9] P. V. Balachandran, B. Kowalski, A. Sehirlioglu, T. Lookman, Experimental search for high-temperature ferroelectric perovskites guided by two-step machine learning, *Nature Communications* 9 (2018) 1668. doi:[10.1038/s41467-018-03821-9](https://doi.org/10.1038/s41467-018-03821-9).
- [10] B. Cao, L. A. Adutwum, A. O. Oliynyk, E. J. Luber, B. C. Olsen, A. Mar, J. M. Buriak, How to optimize materials and devices via design of experiments and machine learning: Demonstration using organic photovoltaics, *ACS Nano* 12 (2018) 7434–7444. doi:[10.1021/acsnano.8b04726](https://doi.org/10.1021/acsnano.8b04726).
- [11] Y. Chen, Y. Tian, Y. Zhou, D. Fang, X. Ding, J. Sun, D. Xue, Machine learning assisted multi-objective optimization for materials processing parameters: A case study in Mg alloy, *Journal of Alloys and Compounds* 844 (2020) 156159. doi:[10.1016/j.jallcom.2020.156159](https://doi.org/10.1016/j.jallcom.2020.156159).
- [12] K. Homma, Y. Liu, M. Sumita, R. Tamura, N. Fushimi, J. Iwata, K. Tsuda, C. Kaneta, Optimization of a Heterogeneous Ternary Li₃PO₄-Li₃BO₃-Li₂SO₄Mixture for Li-Ion Conductivity by Machine Learning, *Journal of Physical Chemistry C* 124 (2020) 12865–12870. doi:[10.1021/acs.jpcc.9b11654](https://doi.org/10.1021/acs.jpcc.9b11654). arXiv:[1911.12576](https://arxiv.org/abs/1911.12576).
- [13] Z. Hou, Y. Takagiwa, Y. Shinohara, Y. Xu, K. Tsuda, Machine-Learning-Assisted Devel-

- opment and Theoretical Consideration for the Al₂Fe₃Si₃ Thermoelectric Material, *ACS Applied Materials and Interfaces* 11 (2019) 11545–11554. doi:[10.1021/acsami.9b02381](https://doi.org/10.1021/acsami.9b02381).
- [14] X. Li, Z. Hou, S. Gao, Y. Zeng, J. Ao, Z. Zhou, B. Da, W. Liu, Y. Sun, Y. Zhang, Efficient Optimization of the Performance of Mn²⁺-Doped Kesterite Solar Cell: Machine Learning Aided Synthesis of High Efficient Cu₂(Mn,Zn)Sn(S,Se)₄ Solar Cells, *Solar RRL* 2 (2018) 1800198. doi:[10.1002/solr.201800198](https://doi.org/10.1002/solr.201800198).
- [15] P. Raccuglia, K. C. Elbert, P. D. Adler, C. Falk, M. B. Wenny, A. Mollo, M. Zeller, S. A. Friedler, J. Schrier, A. J. Norquist, Machine-learning-assisted materials discovery using failed experiments, *Nature* 533 (2016) 73–76. doi:[10.1038/nature17439](https://doi.org/10.1038/nature17439).
- [16] Z. Zhang, A. Mansouri Tehrani, A. O. Oliynyk, B. Day, J. Brgoch, Finding the Next Superhard Material through Ensemble Learning, *Adv. Mater.* 33 (2021) 2005112. doi:[10.1002/adma.202005112](https://doi.org/10.1002/adma.202005112).
- [17] A. Dunn, Q. Wang, A. Ganose, D. Dopp, A. Jain, Benchmarking materials property prediction methods: The Matbench test set and Automatminer reference algorithm, *npj Comput Mater* 6 (2020) 138. doi:[10.1038/s41524-020-00406-3](https://doi.org/10.1038/s41524-020-00406-3).
- [18] Y. Zhuo, A. Mansouri Tehrani, J. Brgoch, Predicting the Band Gaps of Inorganic Solids by Machine Learning, *J. Phys. Chem. Lett.* 9 (2018) 1668–1673. doi:[10.1021/acs.jpcclett.8b00124](https://doi.org/10.1021/acs.jpcclett.8b00124).
- [19] MatBench, <https://matbench.materialsproject.org/>, 2022.
- [20] R. E. A. Goodall, A. A. Lee, Predicting materials properties without crystal structure: Deep representation learning from stoichiometry, *Nat Commun* 11 (2020) 6280. doi:[10.1038/s41467-020-19964-7](https://doi.org/10.1038/s41467-020-19964-7).
- [21] D. Jha, L. Ward, A. Paul, W.-k. Liao, A. Choudhary, C. Wolverton, A. Agrawal, ElemNet: Deep Learning the Chemistry of Materials From Only Elemental Composition, *Sci Rep* 8 (2018) 17593. doi:[10.1038/s41598-018-35934-y](https://doi.org/10.1038/s41598-018-35934-y).
- [22] D. Jha, K. Choudhary, F. Tavazza, W.-k. Liao, A. Choudhary, C. Campbell, A. Agrawal, Enhancing materials property prediction by leveraging computational and experimental data using deep transfer learning, *Nat Commun* 10 (2019) 5316. doi:[10.1038/s41467-019-13297-w](https://doi.org/10.1038/s41467-019-13297-w).
- [23] C. Chen, W. Ye, Y. Zuo, C. Zheng, S. P. Ong, Graph Networks as a Universal Machine Learning Framework for Molecules and Crystals, *Chem. Mater.* 31 (2019) 3564–3572. doi:[10.1021/acs.chemmater.9b01294](https://doi.org/10.1021/acs.chemmater.9b01294).
- [24] P.-P. De Breuck, G. Hautier, G.-M. Rignanese, Materials property prediction for limited datasets enabled by feature selection and joint learning with MODNet, *npj Comput Mater* 7 (2021) 83. doi:[10.1038/s41524-021-00552-2](https://doi.org/10.1038/s41524-021-00552-2).
- [25] M. de Jong, W. Chen, R. Notestine, K. Persson, G. Ceder, A. Jain, M. Asta, A. Gamst, A Statistical Learning Framework for Materials Science: Application to Elastic Moduli of k-nary Inorganic Polycrystalline Compounds, *Sci Rep* 6 (2016) 34256. doi:[10.1038/srep34256](https://doi.org/10.1038/srep34256).
- [26] R. E. A. Goodall, A. S. Parackal, F. A. Faber, R. Armiento, Wyckoff Set Regression for Materials Discovery, in: *Neural Information Processing Systems*, 2020, p. 7.
- [27] J. Klicpera, S. Giri, J. T. Margraf, S. Günemann, Fast and Uncertainty-Aware Directional Message Passing for Non-Equilibrium Molecules, *arXiv:2011.14115 [physics]* (2020). [arXiv:2011.14115](https://arxiv.org/abs/2011.14115).
- [28] S.-Y. Louis, Y. Zhao, A. Nasiri, X. Wang, Y. Song, F. Liu, J. Hu, Graph convolutional

- neural networks with global attention for improved materials property prediction, *Phys. Chem. Chem. Phys.* 22 (2020) 18141–18148. doi:[10.1039/D0CP01474E](https://doi.org/10.1039/D0CP01474E).
- [29] C. W. Park, C. Wolverton, Developing an improved crystal graph convolutional neural network framework for accelerated materials discovery, *Phys. Rev. Materials* 4 (2020) 063801. doi:[10.1103/PhysRevMaterials.4.063801](https://doi.org/10.1103/PhysRevMaterials.4.063801).
- [30] T. Xie, J. C. Grossman, Crystal Graph Convolutional Neural Networks for an Accurate and Interpretable Prediction of Material Properties, *Phys. Rev. Lett.* 120 (2018) 145301. doi:[10.1103/PhysRevLett.120.145301](https://doi.org/10.1103/PhysRevLett.120.145301).
- [31] D. Eriksson, M. Jankowiak, High-Dimensional Bayesian Optimization with Sparse Axis-Aligned Subspaces, arXiv:2103.00349 [cs, stat] (2021). [arXiv:2103.00349](https://arxiv.org/abs/2103.00349).
- [32] High-Dimensional Bayesian Optimization with SAASBO, <https://ax.dev/tutorials/saasbo.html>, 2022.
- [33] Y. Chung, I. Char, H. Guo, J. Schneider, W. Neiswanger, Uncertainty Toolbox: An Open-Source Library for Assessing, Visualizing, and Improving Uncertainty Quantification, arXiv:2109.10254 [cs, stat] (2021). [arXiv:2109.10254](https://arxiv.org/abs/2109.10254).
- [34] Citrine Informatics: AI-Powered Materials Data Platform, <https://citrination.com/>, 2022.
- [35] S. G. Baird, T. Q. Diep, T. D. Sparks, DiS-CoVeR: A Materials Discovery Screening Tool for High Performance, Unique Chemical Compositions, *Digital Discovery* (2022). doi:[10.1039/D1DD00028D](https://doi.org/10.1039/D1DD00028D).
- [36] P. T. Inc., Collaborative data science, <https://plot.ly>, 2015.
- [37] Create LaTeX tables online – TablesGenerator.com, <https://www.tablesgenerator.com/>, 2021.
- [38] Auto-paper, sparks-baird, 2021.
- [39] S. Baird, sgbaire-alt, mliu7051, Sparks-baird/crabnet-hyperparameter:, Zenodo, 2022. doi:[10.5281/zenodo.6355045](https://doi.org/10.5281/zenodo.6355045).

High-dimensional Bayesian Optimization of Hyperparameters for an Attention-based Network to Predict Materials Property: a Case Study on CrabNet using Ax and SAASBO: Supporting Information

Sterling G. Baird^{a,*}, Marianne Liu^{a,b}, Taylor D. Sparks^a

^a*Department of Materials Science and Engineering, University of Utah, Salt Lake City, UT 84108, USA*

^b*West High School, Salt Lake City, Utah 84112, USA*

arXiv:2203.12597v1 [cond-mat.mtrl-sci] 19 Mar 2022

Contents

S1 Fold-wise Feature Importances **1**

S2 1D Slices through Model Parameter Space **4**

S1. Fold-wise Feature Importances

Feature importances for each of the 5 Matbench folds across the 23 hyperparameters for the Gaussian process expected improvement (GPEI) and sparse axis-aligned subspaces Bayesian optimization models (SAASBO) are given in [Figure S1](#) and [Figure S2](#), respectively.

*Corresponding author.

Email addresses: sterling.baird@utah.edu (Sterling G. Baird), sparks@eng.utah.edu (Taylor D. Sparks)

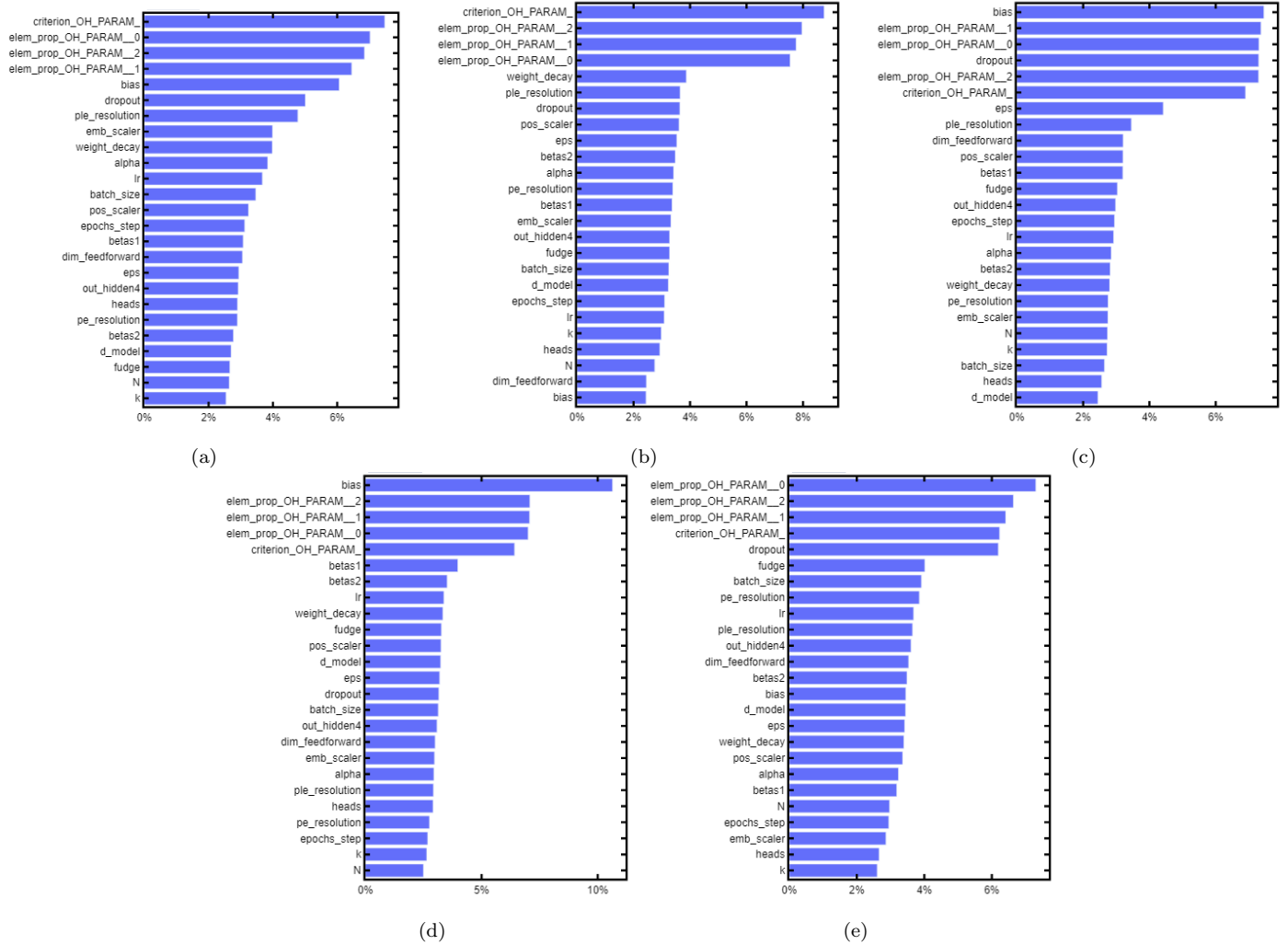


Figure S1: Relative GPEI feature importances of Compositionally-Restricted Attention-Based Network hyperparameters for each of the five `matbench_expt_gap` folds based on data from 100 iterations. `_OH_PARAM_#` refers to choices for categorical variables. The first 46 iterations were Sobol points, and the remaining 54 iterations were Bayesian optimization iterations.

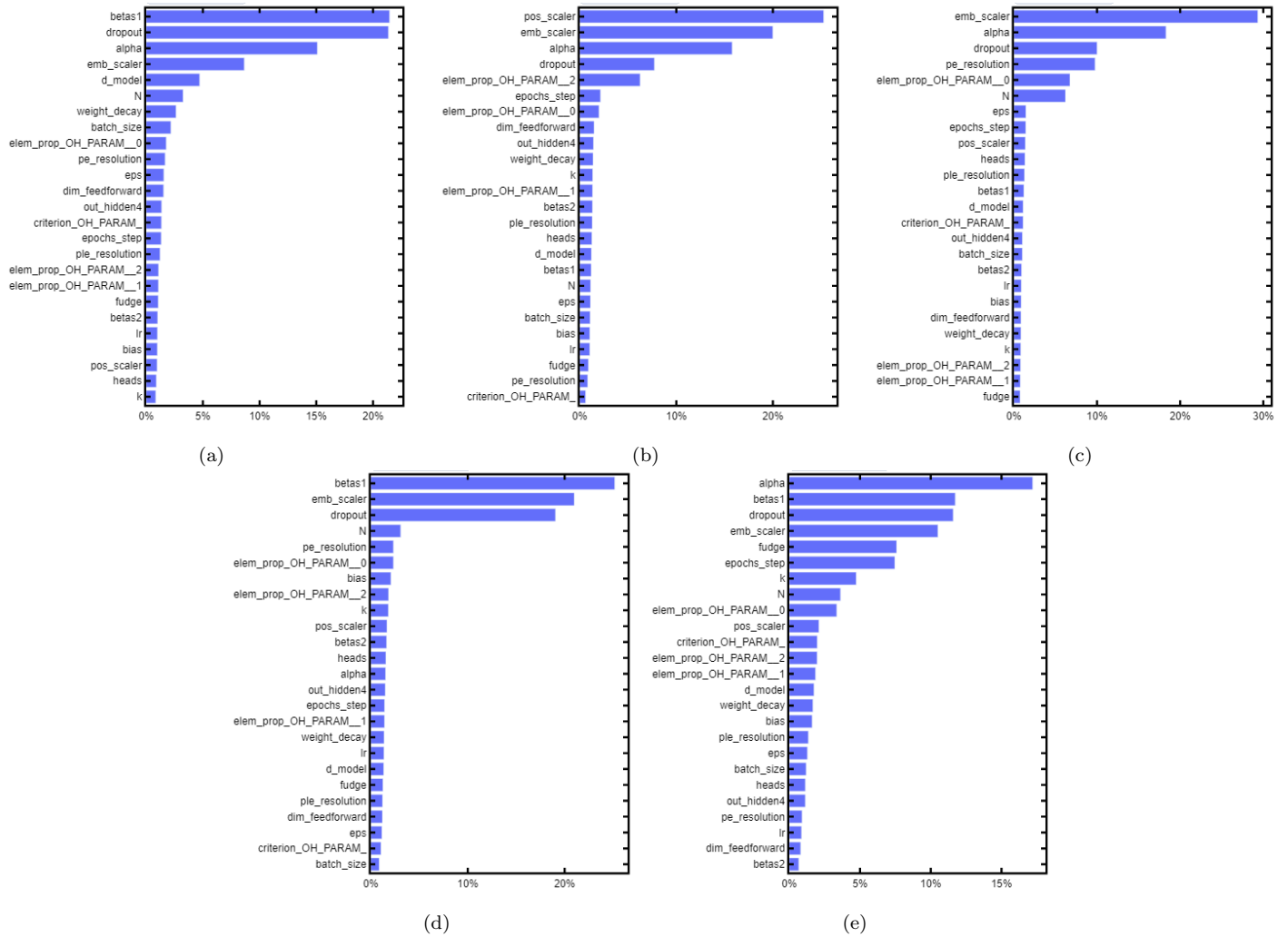


Figure S2: Relative SAASBO feature importances of Compositionally-Restricted Attention-Based Network hyperparameters for each of the five `matbench_expt_gap` folds based on data from 100 iterations. `_OH_PARAM_#` refers to choices for categorical variables. The first 10 iterations were Sobol points, and the remaining 90 were sparse axis-aligned subspaces Bayesian optimization iterations. Note that feature importances are tied with the constraints on the search space imposed by the user. A differently constrained search space (and by extension characteristics of the sampled points) may result in different feature importances.

S2. 1D Slices through Model Parameter Space

One-dimensional slices through GPEI (top row) and SAASBO (bottom row) models for each of the 23 CrabNet hyperparameters (??) and for each of the 5 Matbench folds are shown following roughly the order in ??. There is one figure per hyperparameter, labeled above each figure as well as mentioned within the caption.

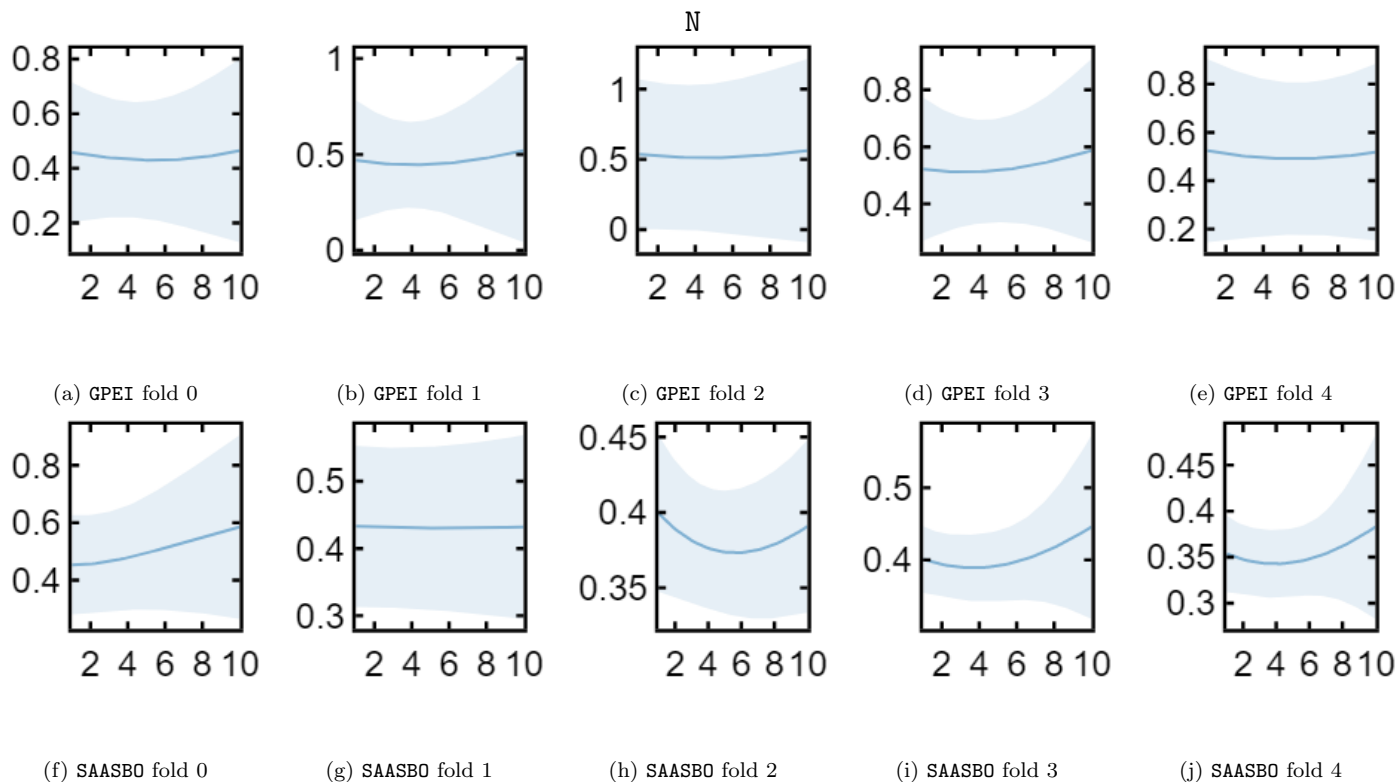


Figure S3: One-dimensional (1D) slices of mean absolute error (MAE) (eV) vs. N through the GPEI and SAASBO parameter spaces with the rest of the parameters fixed to the mean and mode of the numeric and categorical parameters for each of the models, respectively. Shaded blue error bands give the standard deviation uncertainty predicted by the model. .

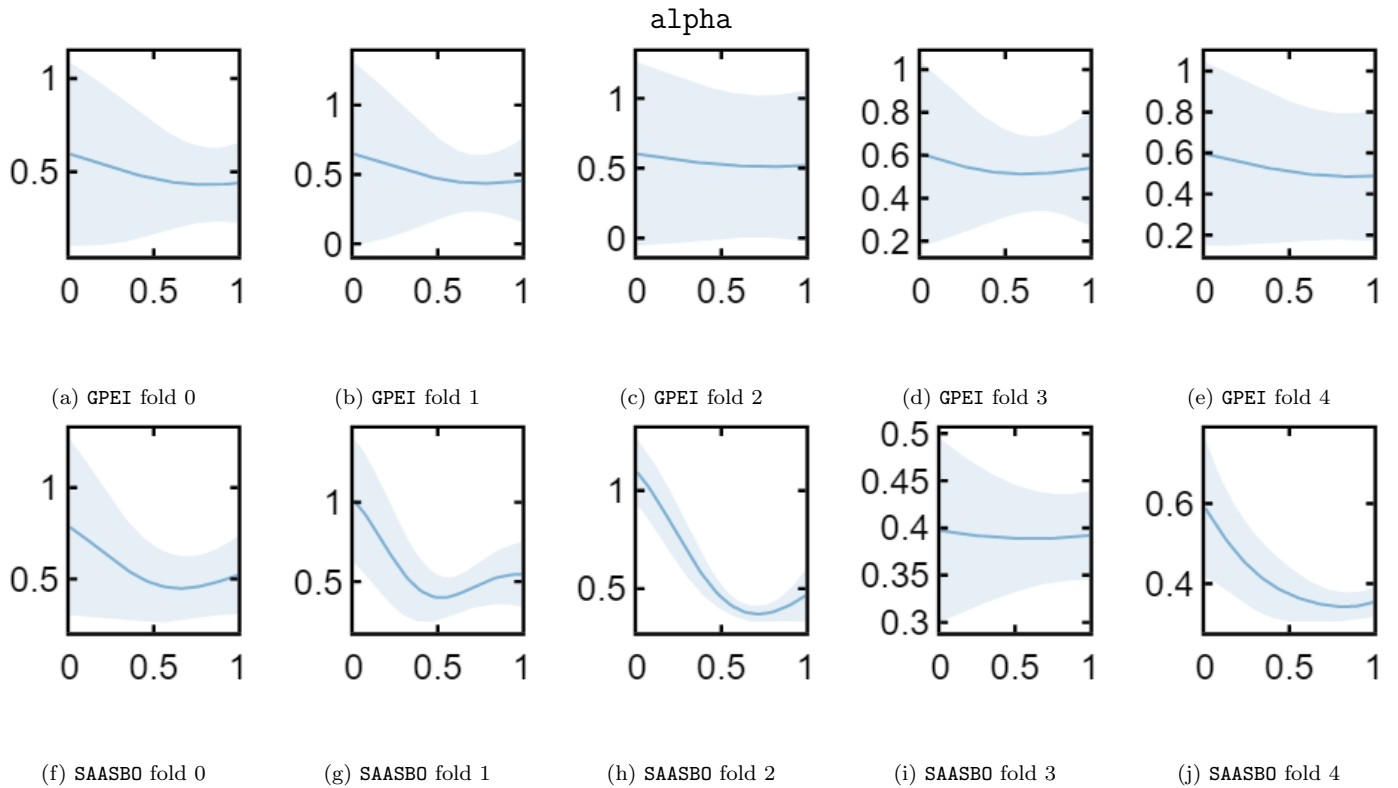


Figure S4: One-dimensional (1D) slices of MAE (eV) vs. `alpha` through the GPEI and SAASBO parameter spaces with the rest of the parameters fixed to the mean and mode of the numeric and categorical parameters for each of the models, respectively. Shaded blue error bands give the standard deviation uncertainty predicted by the model. .

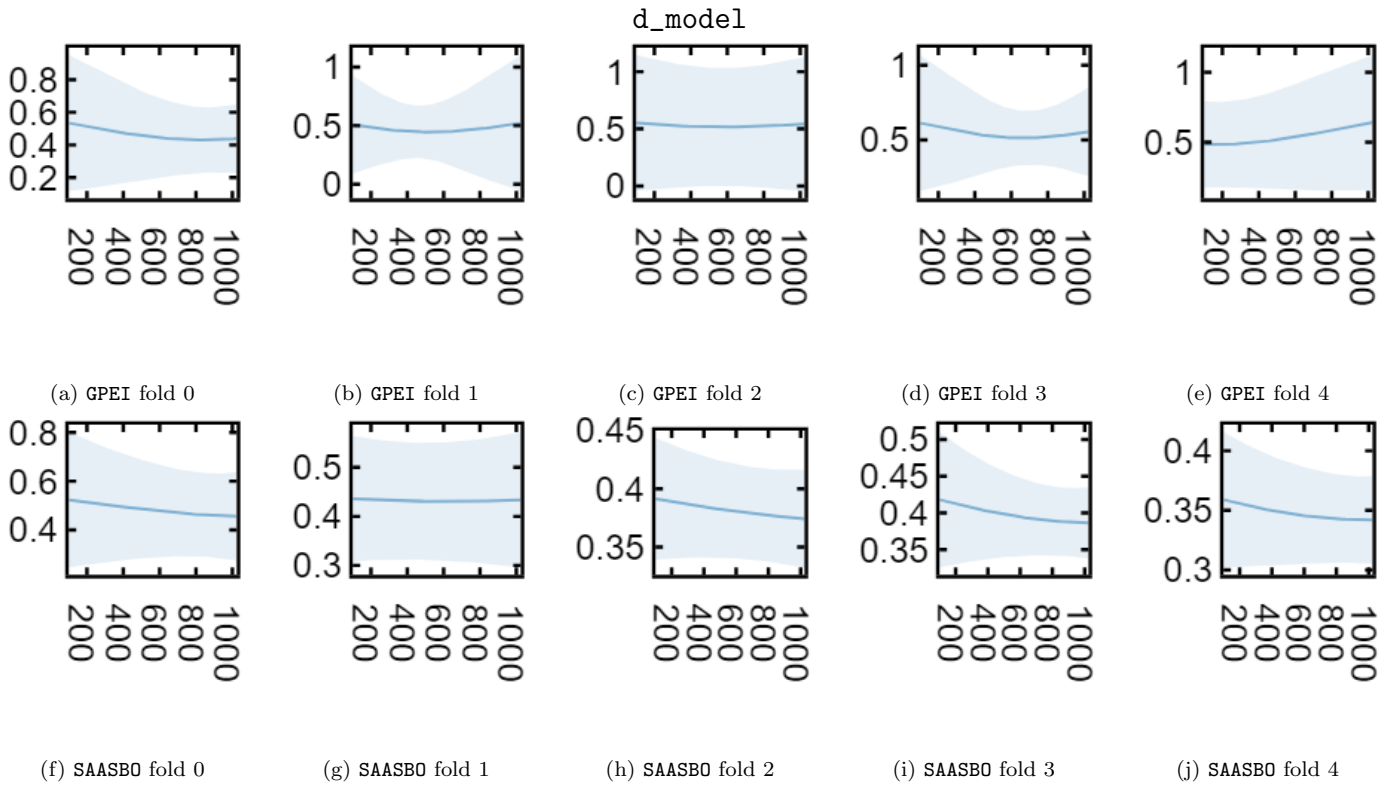


Figure S5: One-dimensional (1D) slices of MAE (eV) vs. `d_model` through the GPEI and SAASBO parameter spaces with the rest of the parameters fixed to the mean and mode of the numeric and categorical parameters for each of the models, respectively. Shaded blue error bands give the standard deviation uncertainty predicted by the model. .

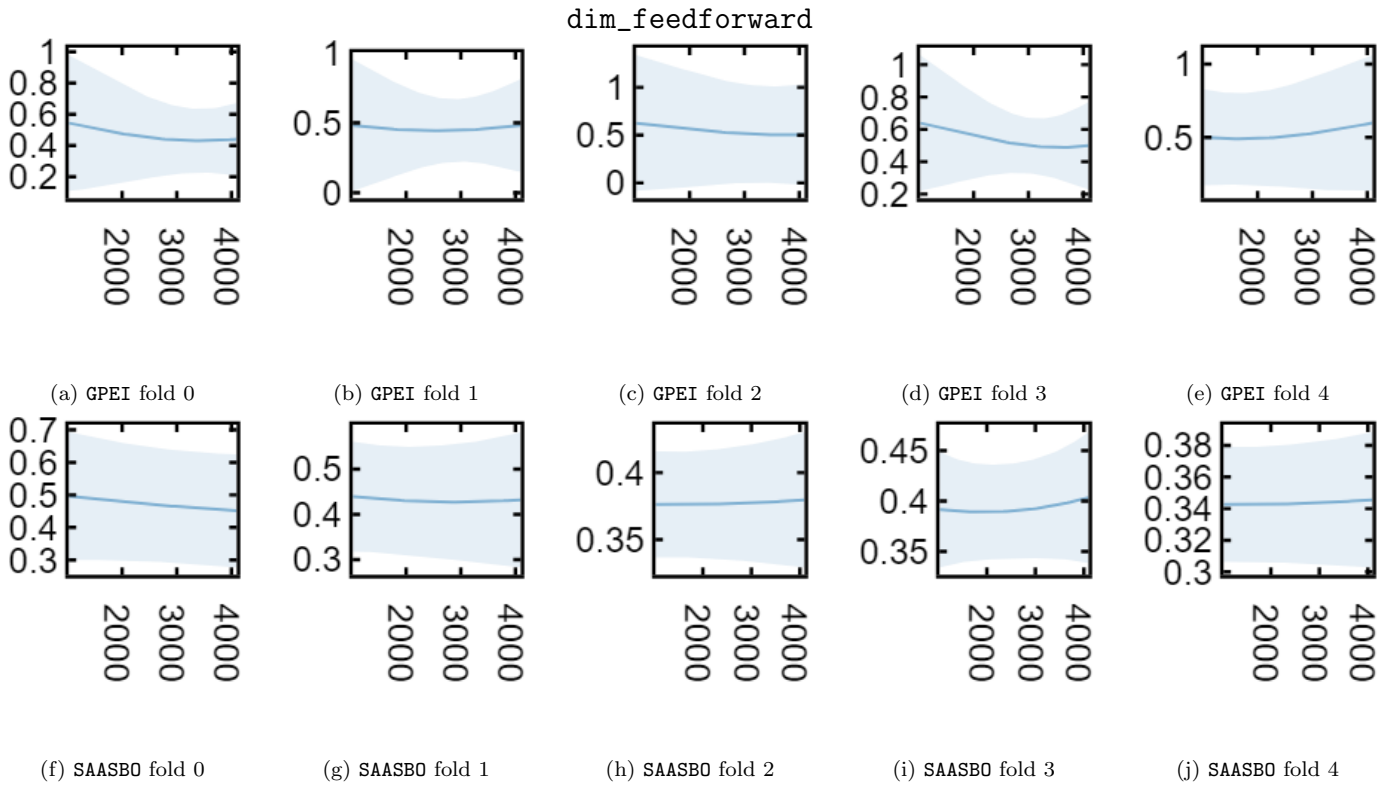


Figure S6: One-dimensional (1D) slices of MAE (eV) vs. `dim_feedforward` through the GPEI and SAASBO parameter spaces with the rest of the parameters fixed to the mean and mode of the numeric and categorical parameters for each of the models, respectively. Shaded blue error bands give the standard deviation uncertainty predicted by the model. .

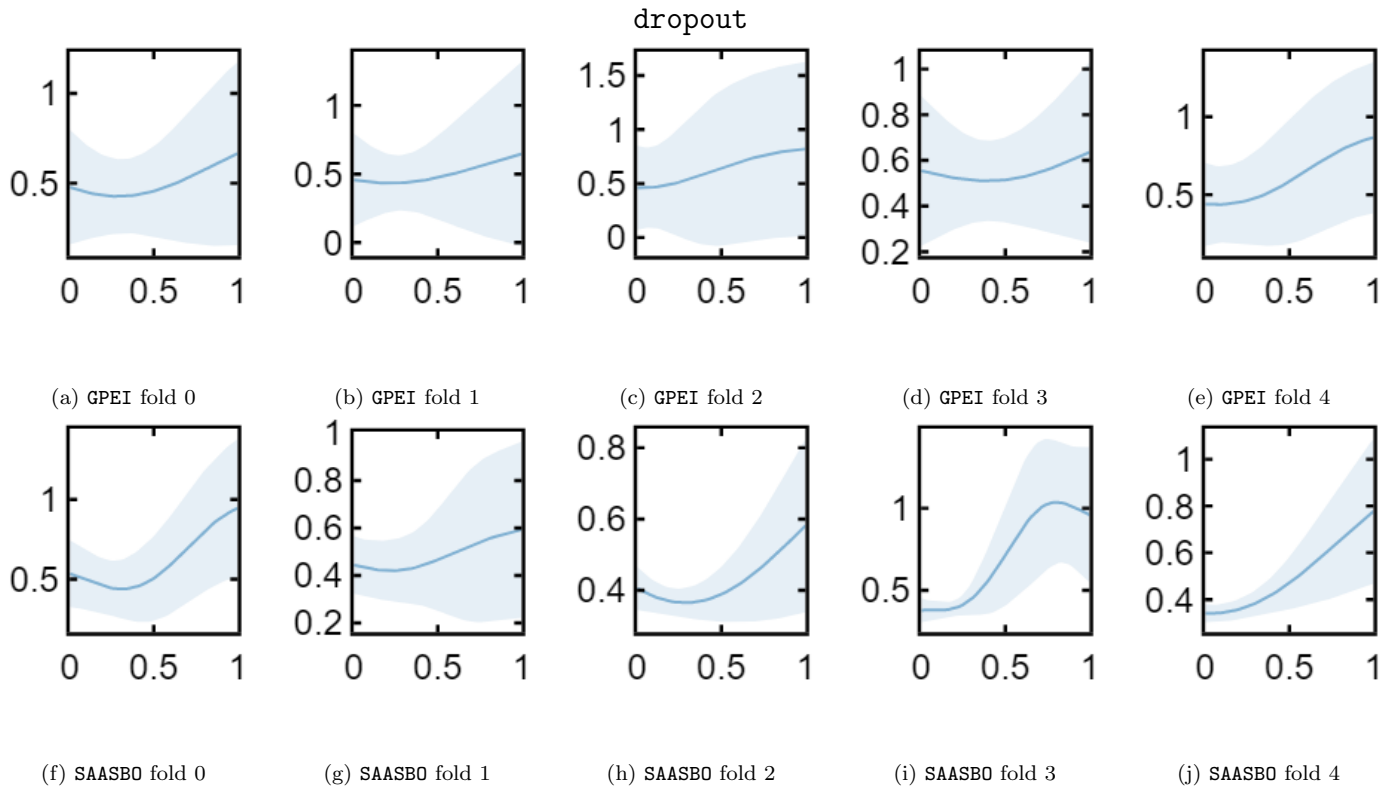


Figure S7: One-dimensional (1D) slices of MAE (eV) vs. dropout through the GPEI and SAASBO parameter spaces with the rest of the parameters fixed to the mean and mode of the numeric and categorical parameters for each of the models, respectively. Shaded blue error bands give the standard deviation uncertainty predicted by the model. .

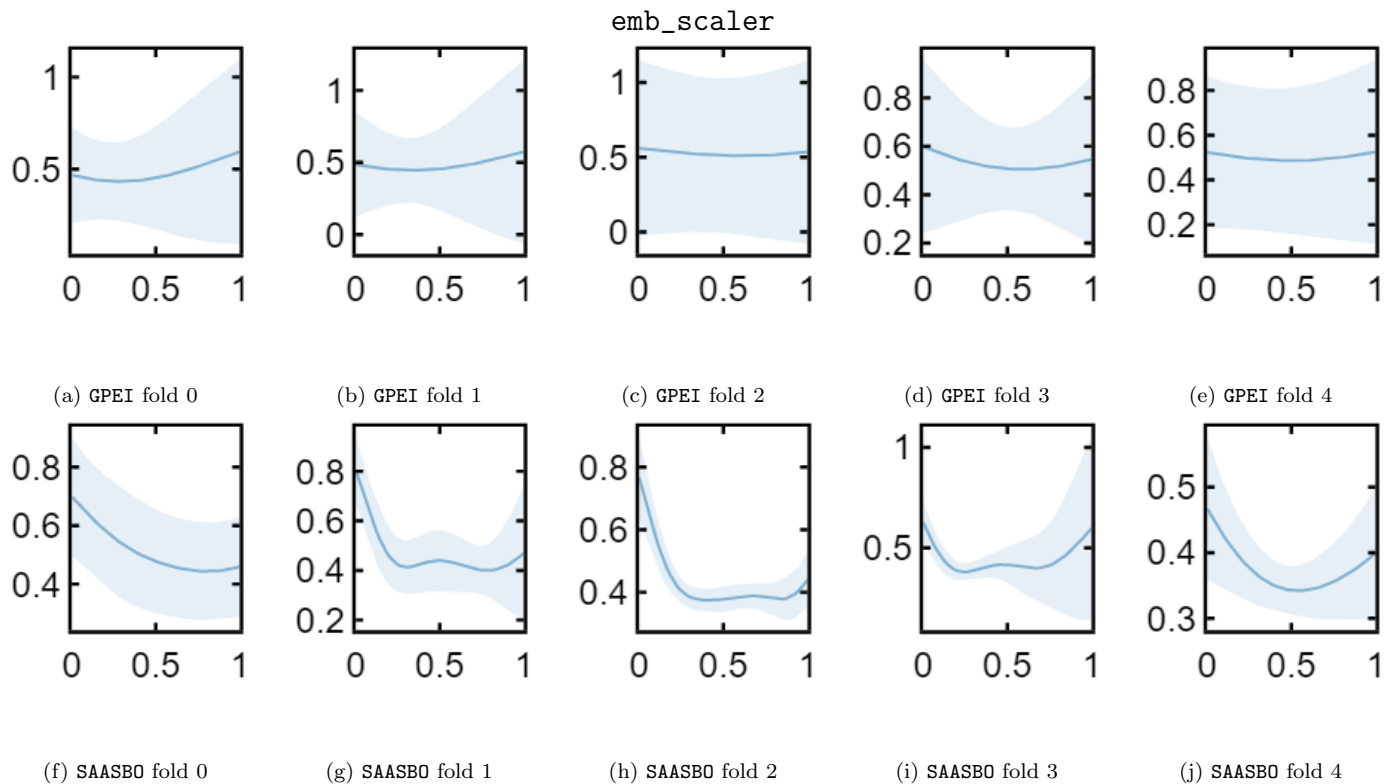


Figure S8: One-dimensional (1D) slices of MAE (eV) vs. `emb_scaler` through the GPEI and SAASBO parameter spaces with the rest of the parameters fixed to the mean and mode of the numeric and categorical parameters for each of the models, respectively. Shaded blue error bands give the standard deviation uncertainty predicted by the model. .

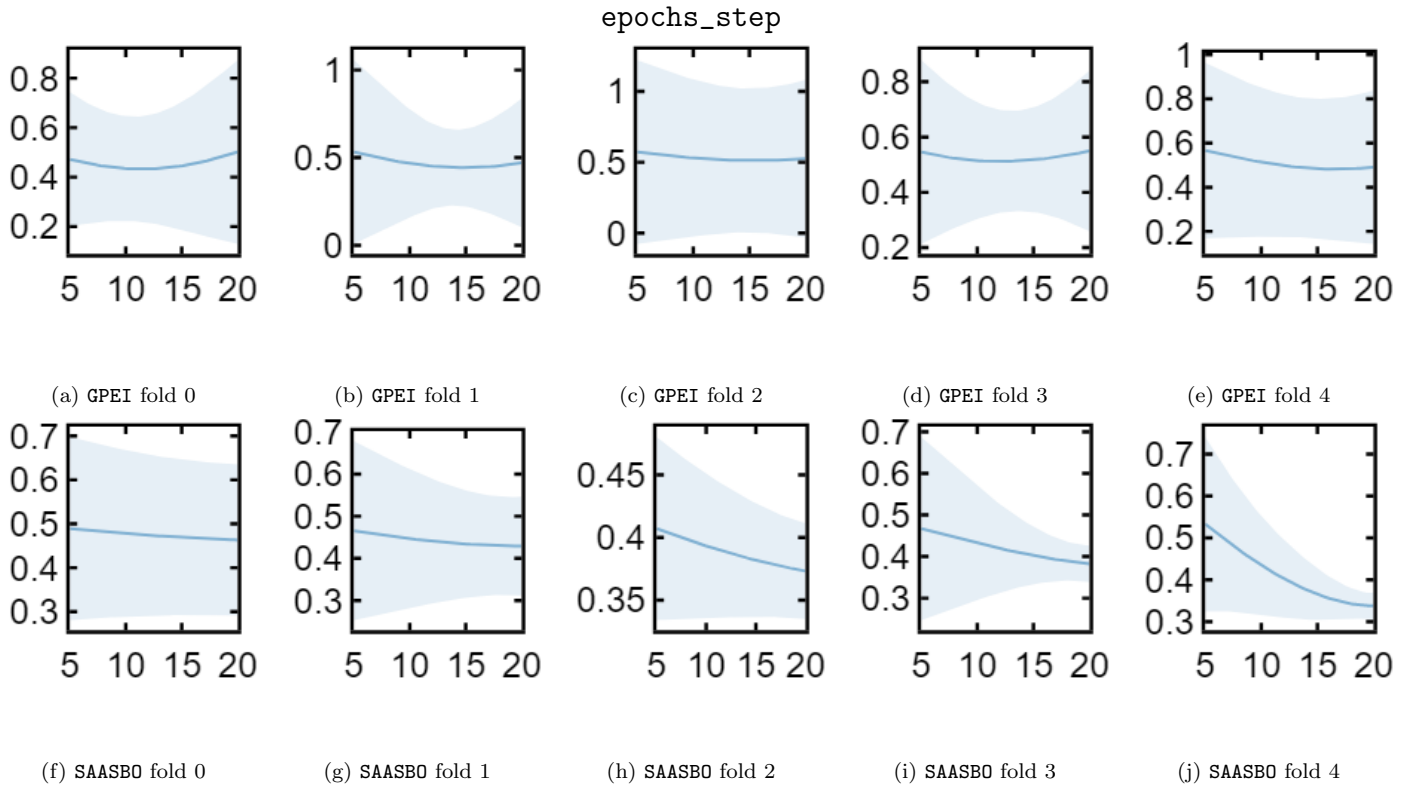


Figure S9: One-dimensional (1D) slices of MAE (eV) vs. `epochs_step` through the GPEI and SAASBO parameter spaces with the rest of the parameters fixed to the mean and mode of the numeric and categorical parameters for each of the models, respectively. Shaded blue error bands give the standard deviation uncertainty predicted by the model. .

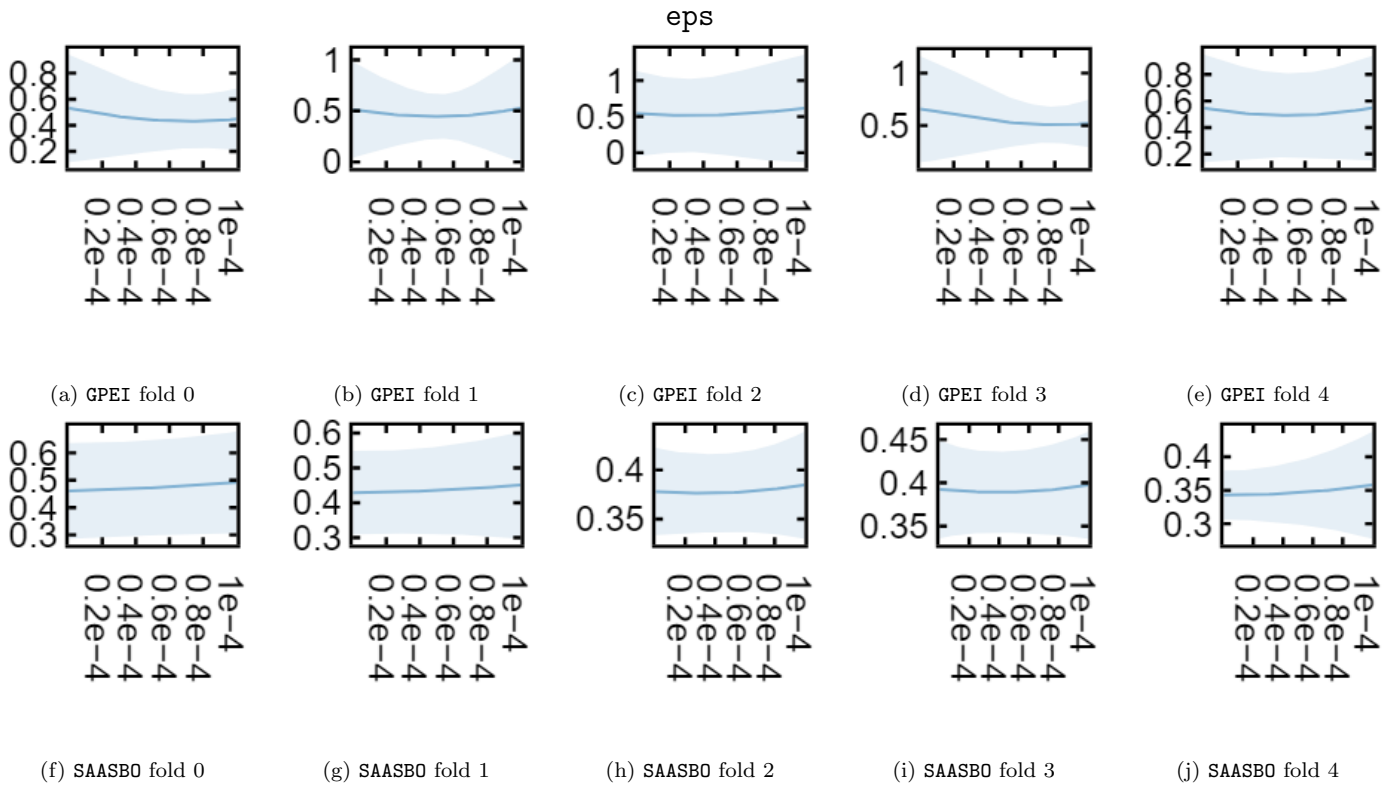


Figure S10: One-dimensional (1D) slices of MAE (eV) vs. `eps` through the GPEI and SAASBO parameter spaces with the rest of the parameters fixed to the mean and mode of the numeric and categorical parameters for each of the models, respectively. Shaded blue error bands give the standard deviation uncertainty predicted by the model. .

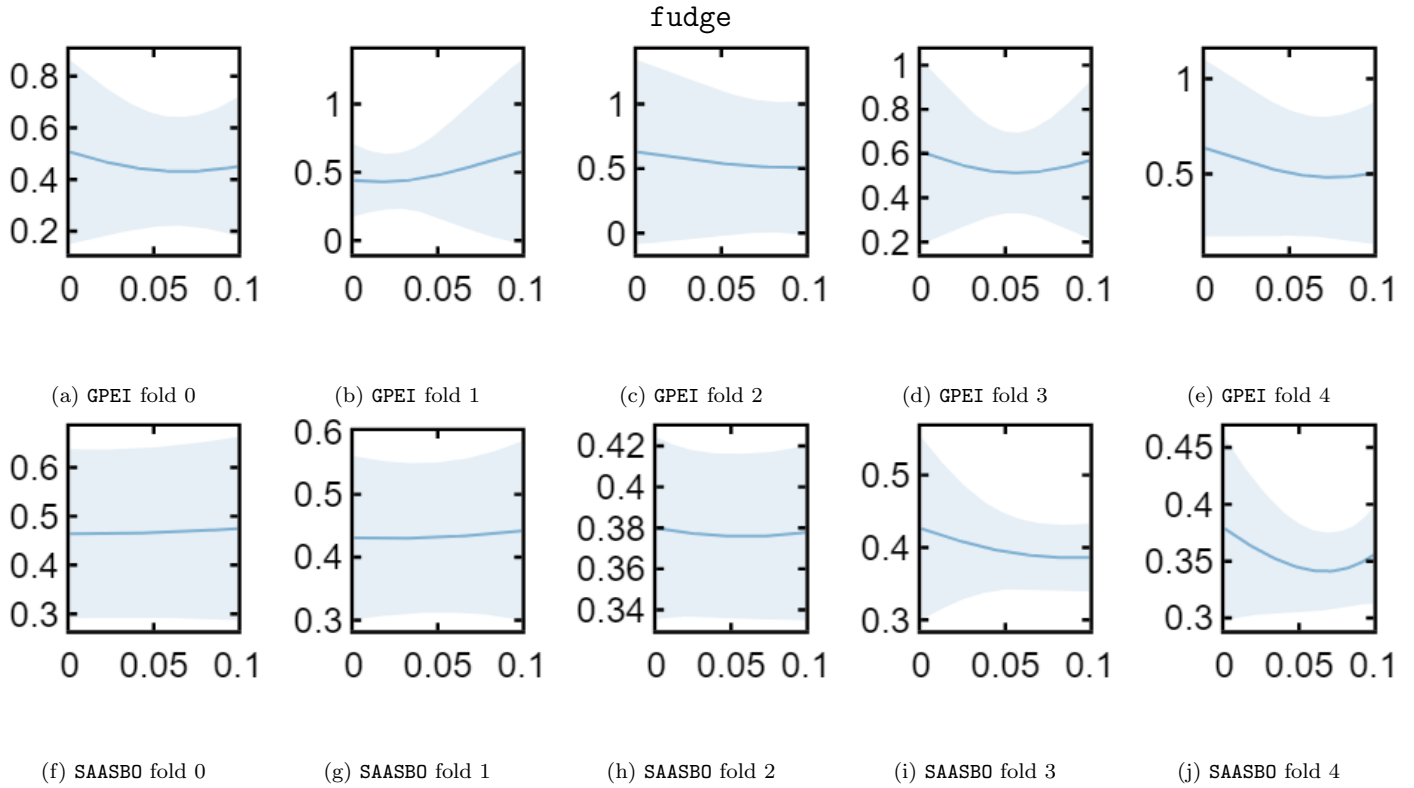


Figure S11: One-dimensional (1D) slices of MAE (eV) vs. `fudge` through the GPEI and SAASBO parameter spaces with the rest of the parameters fixed to the mean and mode of the numeric and categorical parameters for each of the models, respectively. Shaded blue error bands give the standard deviation uncertainty predicted by the model. .

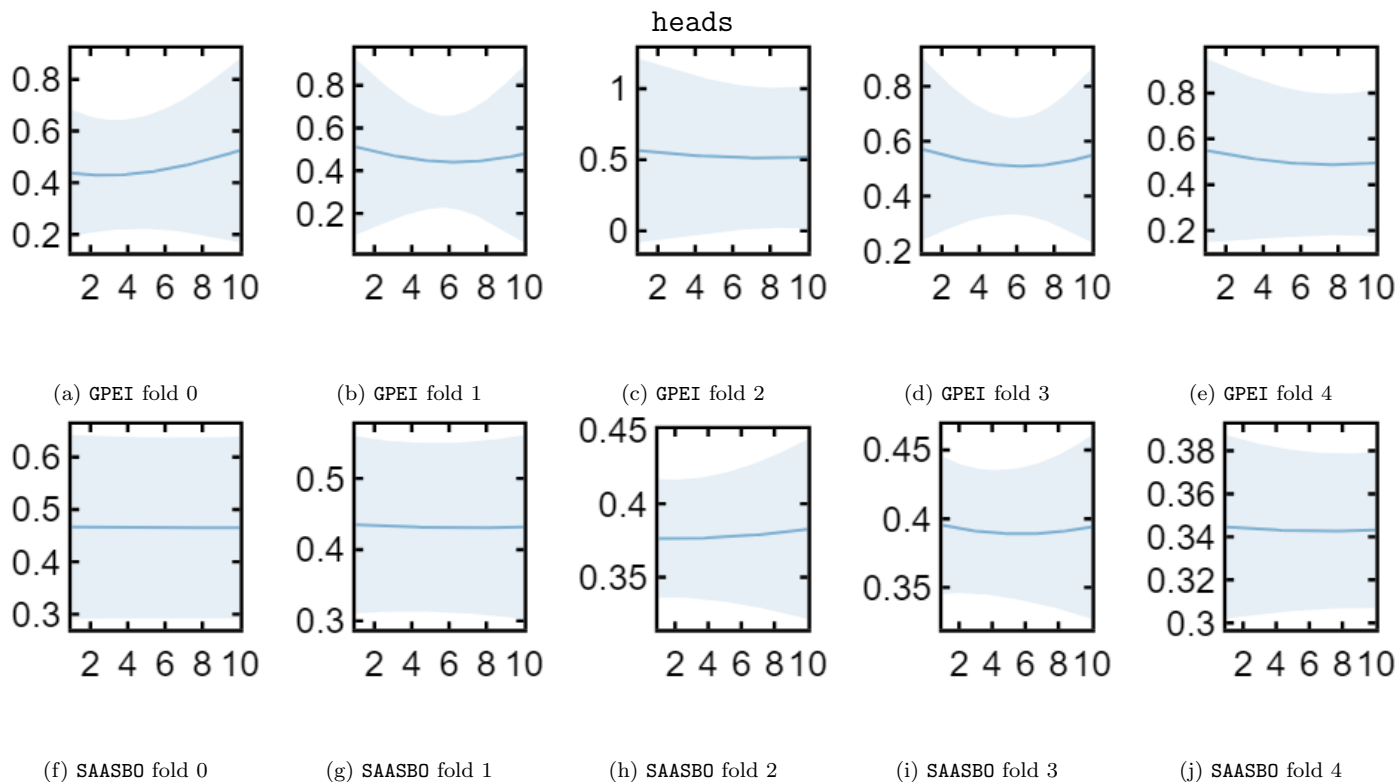


Figure S12: One-dimensional (1D) slices of MAE (eV) vs. `heads` through the GPEI and SAASBO parameter spaces with the rest of the parameters fixed to the mean and mode of the numeric and categorical parameters for each of the models, respectively. Shaded blue error bands give the standard deviation uncertainty predicted by the model. .

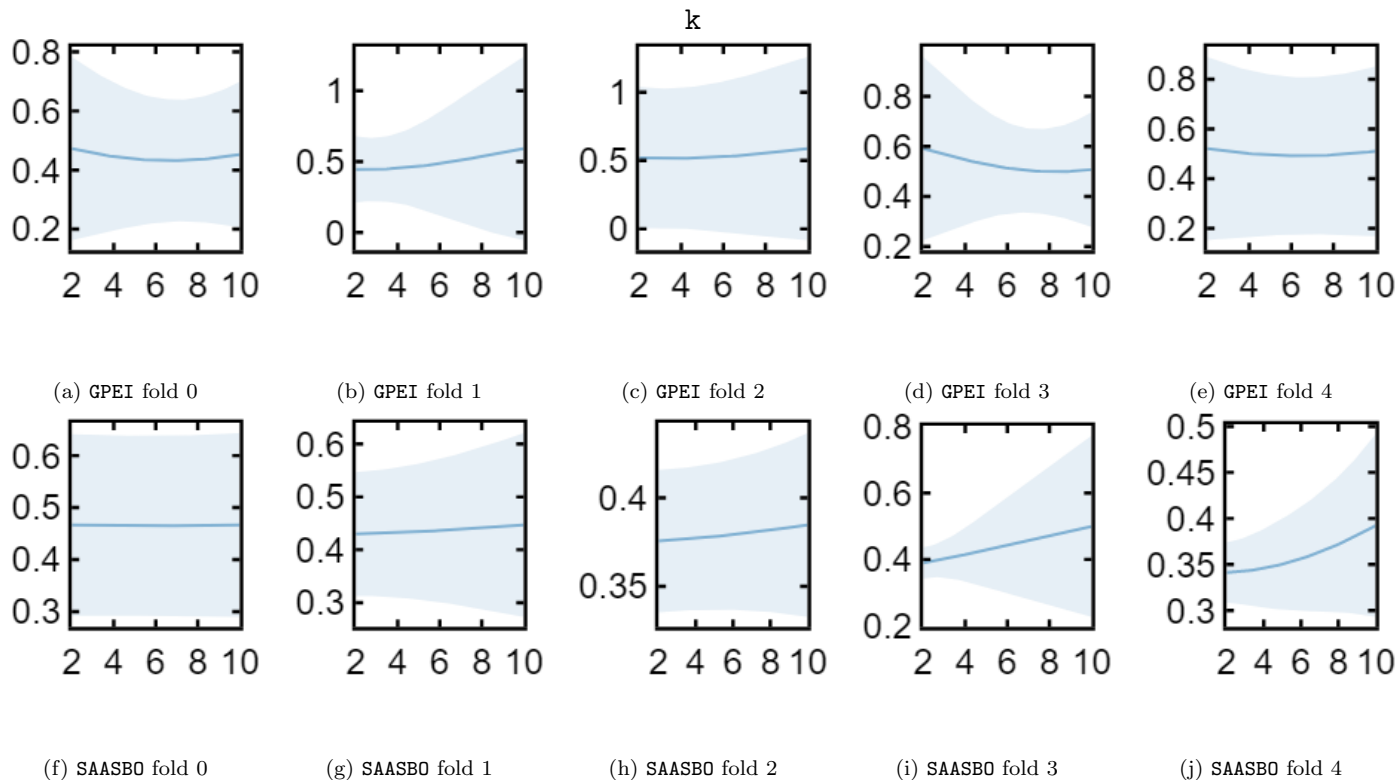


Figure S13: One-dimensional (1D) slices of MAE (eV) vs. k through the GPEI and SAASBO parameter spaces with the rest of the parameters fixed to the mean and mode of the numeric and categorical parameters for each of the models, respectively. Shaded blue error bands give the standard deviation uncertainty predicted by the model. .

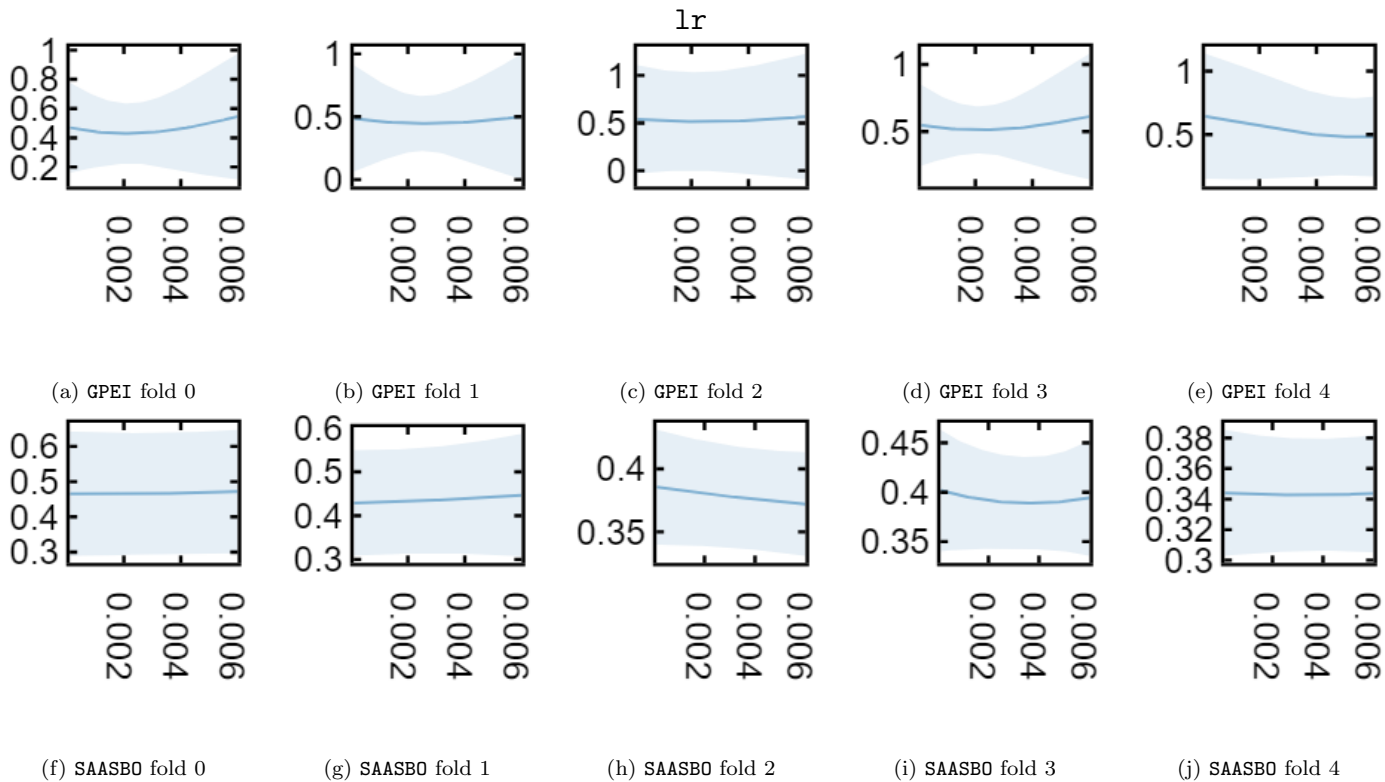


Figure S14: One-dimensional (1D) slices of MAE (eV) vs. lr through the GPEI and SAASBO parameter spaces with the rest of the parameters fixed to the mean and mode of the numeric and categorical parameters for each of the models, respectively. Shaded blue error bands give the standard deviation uncertainty predicted by the model. .

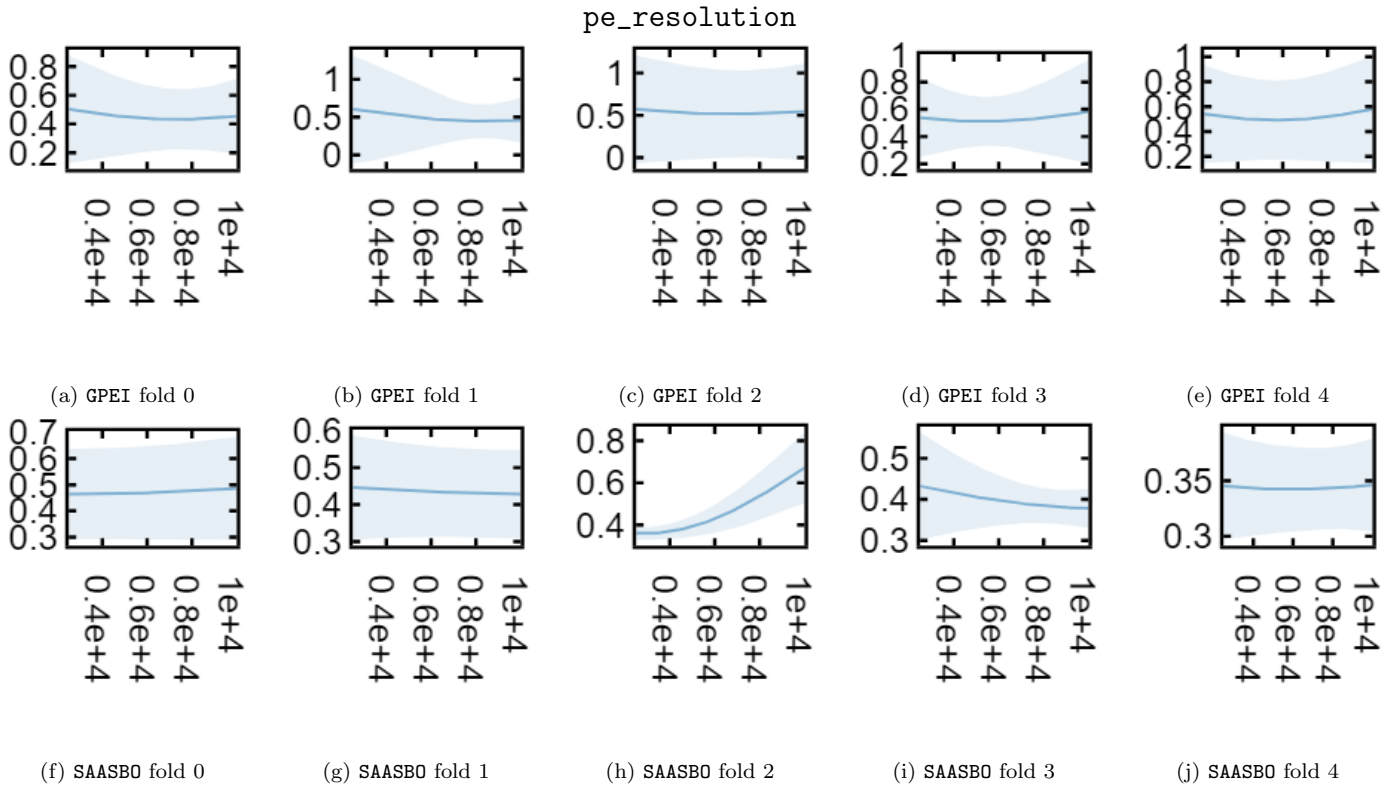


Figure S15: One-dimensional (1D) slices of MAE (eV) vs. `pe_resolution` through the GPEI and SAASBO parameter spaces with the rest of the parameters fixed to the mean and mode of the numeric and categorical parameters for each of the models, respectively. Shaded blue error bands give the standard deviation uncertainty predicted by the model. .

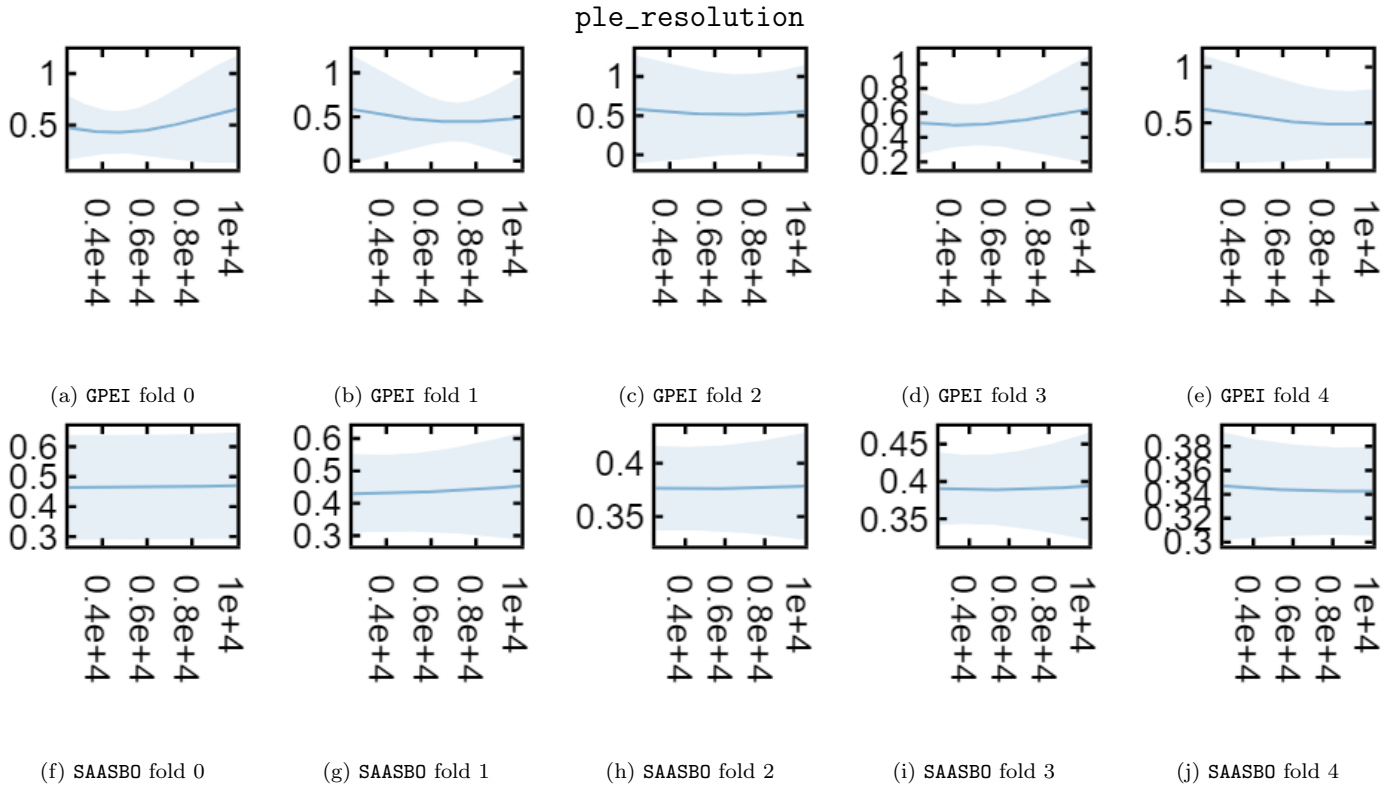


Figure S16: One-dimensional (1D) slices of MAE (eV) vs. `ple_resolution` through the GPEI and SAASBO parameter spaces with the rest of the parameters fixed to the mean and mode of the numeric and categorical parameters for each of the models, respectively. Shaded blue error bands give the standard deviation uncertainty predicted by the model. .

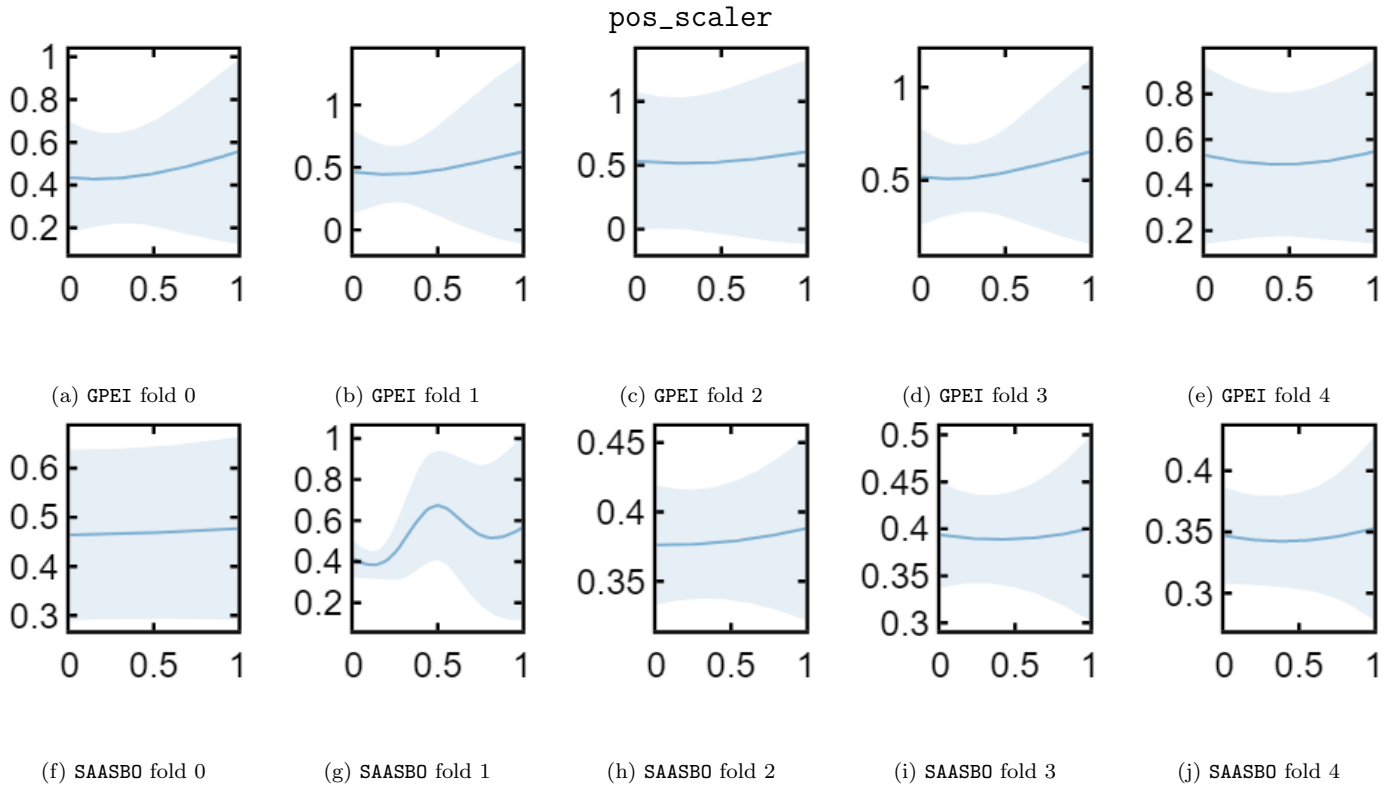


Figure S17: One-dimensional (1D) slices of MAE (eV) vs. `pos_scaler` through the GPEI and SAASBO parameter spaces with the rest of the parameters fixed to the mean and mode of the numeric and categorical parameters for each of the models, respectively. Shaded blue error bands give the standard deviation uncertainty predicted by the model. .

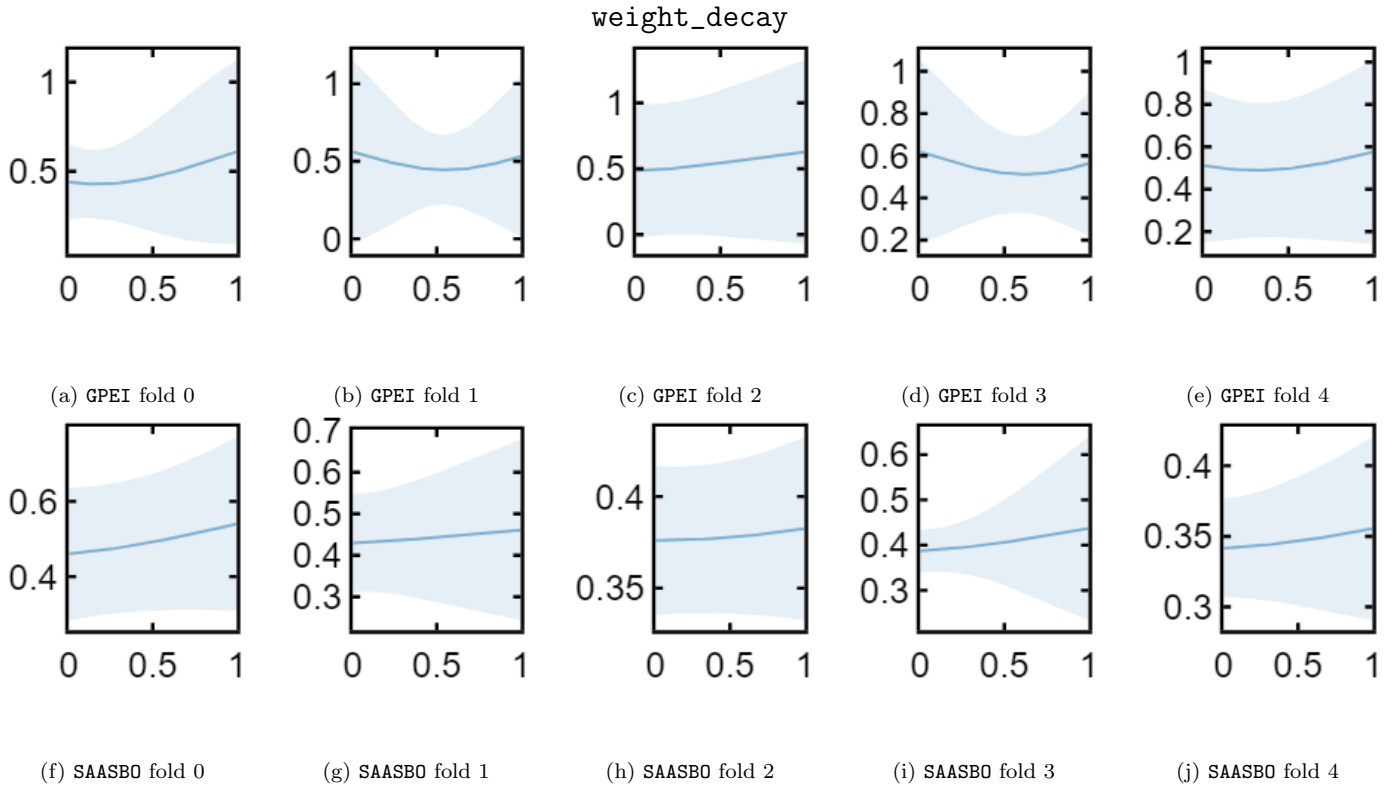


Figure S18: One-dimensional (1D) slices of MAE (eV) vs. `weight_decay` through the GPEI and SAASBO parameter spaces with the rest of the parameters fixed to the mean and mode of the numeric and categorical parameters for each of the models, respectively. Shaded blue error bands give the standard deviation uncertainty predicted by the model. .

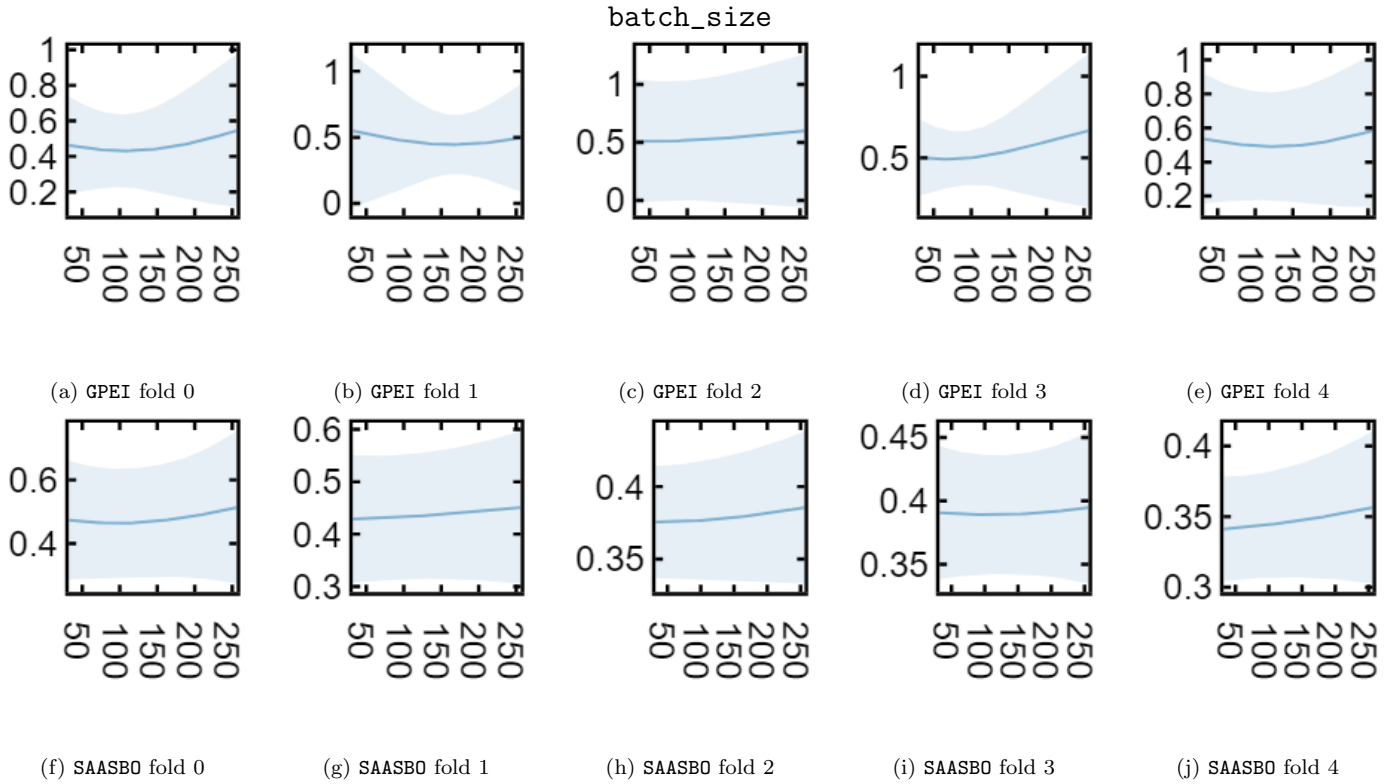


Figure S19: One-dimensional (1D) slices of MAE (eV) vs. `batch_size` through the GPEI and SAASBO parameter spaces with the rest of the parameters fixed to the mean and mode of the numeric and categorical parameters for each of the models, respectively. Shaded blue error bands give the standard deviation uncertainty predicted by the model. .

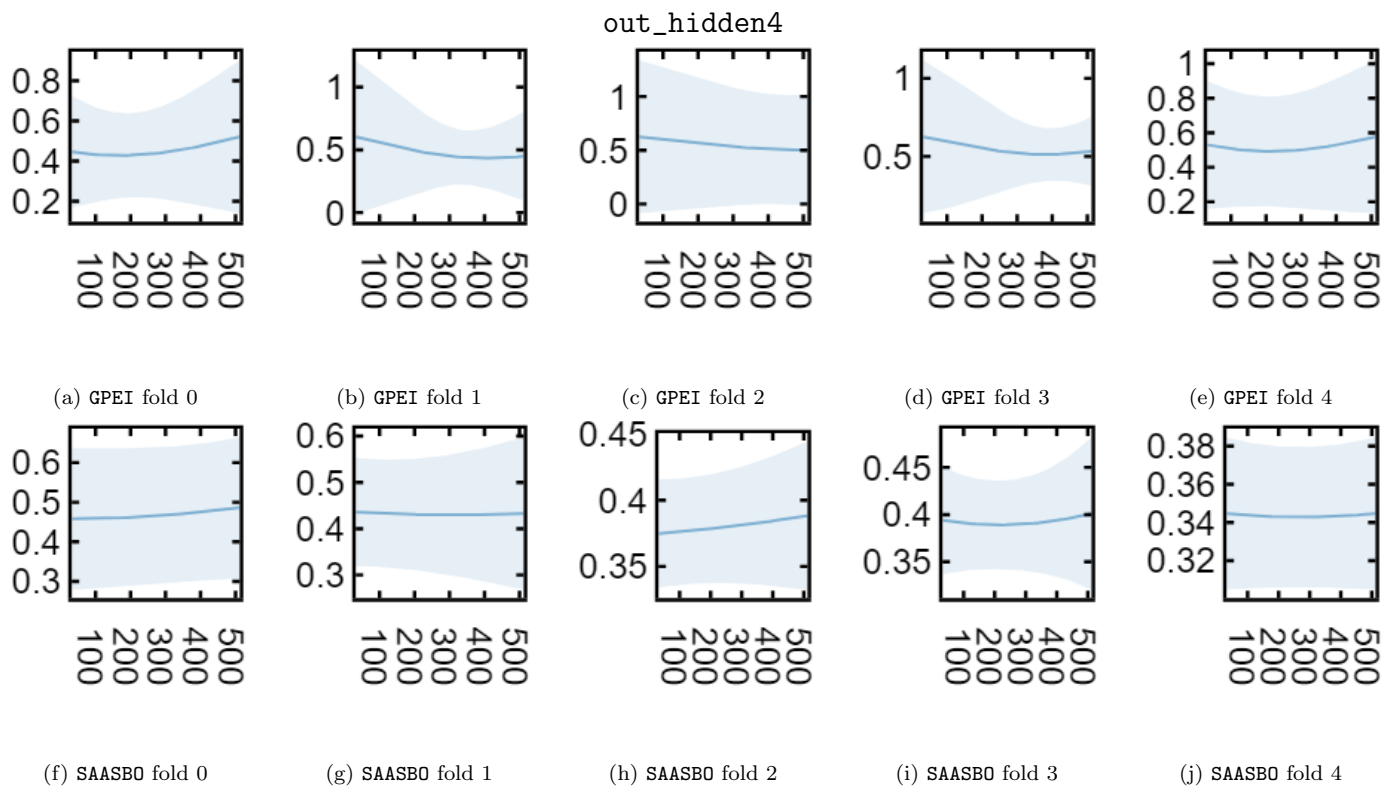


Figure S20: One-dimensional (1D) slices of MAE (eV) vs. `out_hidden4` through the GPEI and SAASBO parameter spaces with the rest of the parameters fixed to the mean and mode of the numeric and categorical parameters for each of the models, respectively. Shaded blue error bands give the standard deviation uncertainty predicted by the model. .

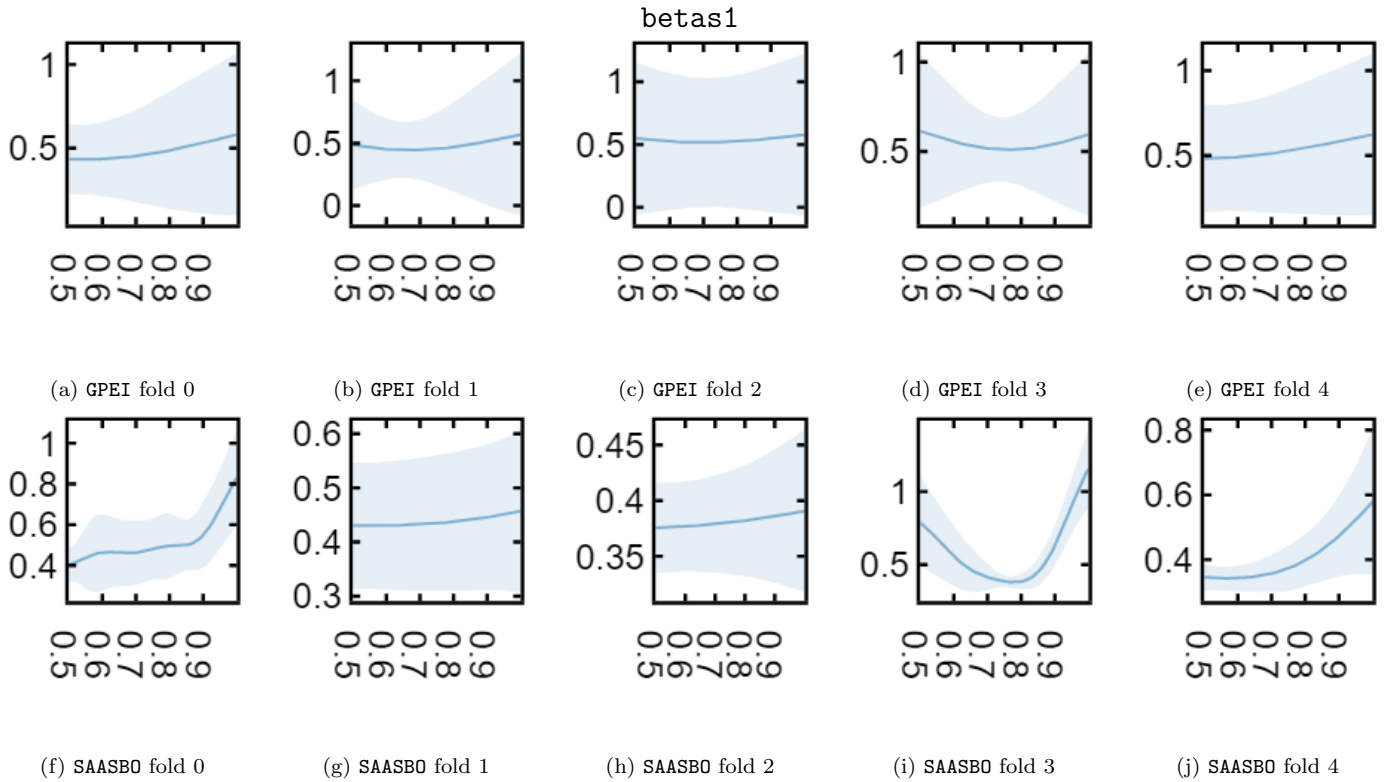


Figure S21: One-dimensional (1D) slices of MAE (eV) vs. `betas1` through the GPEI and SAASBO parameter spaces with the rest of the parameters fixed to the mean and mode of the numeric and categorical parameters for each of the models, respectively. Shaded blue error bands give the standard deviation uncertainty predicted by the model. .

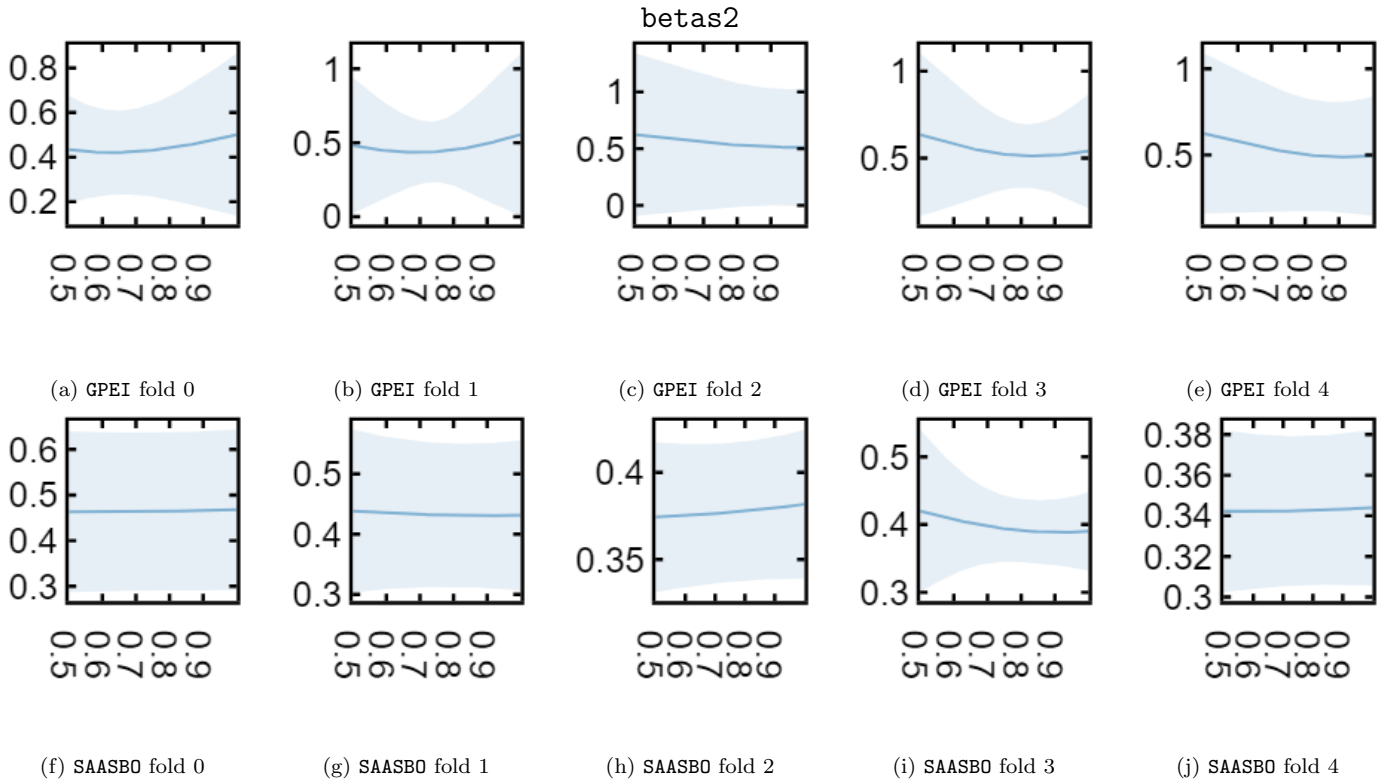


Figure S22: One-dimensional (1D) slices of MAE (eV) vs. `betas2` through the GPEI and SAASBO parameter spaces with the rest of the parameters fixed to the mean and mode of the numeric and categorical parameters for each of the models, respectively. Shaded blue error bands give the standard deviation uncertainty predicted by the model. .